Exploring the Limits of Mapping Seagrass

A case study for *P. oceanica*

Sylvia Noralez

March, 2010

Exploring the Limits of Mapping Seagrass

A case study of *P. oceanica*

by

Sylvia Noralez

Thesis submitted to the International Institute for Geo-information Science and Earth Observation in partial fulfilment of the requirements for the degree of Master of Science in Geo-information Science and Earth Observation, Specialisation: Natural Resource Management

Thesis Assessment Board

Chair	: Dr. A.G. Toxopeus (Department of Natural Resource Department, ITC)
External Examiner	: Dr. P. Lymberakis (Department of Zoology, University of Crete)
First Supervisor	: Drs. Valentyn Venus (Department of Natural Resource Department, ITC)
Supervisors	: Drs. Valentyn Venus (Department of Natural Resource Department, ITC)
	: Dr. Martin Schlerf (Department of Natural Resource Department, ITC)

INTERNATIONAL INSTITUTE FOR GEO-INFORMATION SCIENCE AND EARTH OBSERVATION
ENSCHEDE, THE NETHERLANDS

Disclaimer

This document describes work undertaken as part of a programme of study at the International Institute for Geo-information Science and Earth Observation. All views and opinions expressed therein remain the sole responsibility of the author, and do not necessarily represent those of the institute.

Abstract

Effective identification and mapping of seagrass communities using high spatial and spectral resolution digital imaging spectroscopy are distinguishable by their spectral reflectance characteristics. Hence determining a sunset of wavelength that best discriminates *P. oceanica* from other seafloor types is essential for development of remote sensing techniques to monitor them. The study measure spectral reflectance of *P. oceanica* and carbonate sand in the Agia Pelagia Bay, Crete, Greece on a bright sunny day. Laboratory measurements were also conducted. The *in situ* and laboratory data was spectrally distinct form other seafloor types within the visible spectral range of the spectrum. We compared the results from other to other research and found that the *P. oceanica* was spectrally distinct within the visible range of the spectrum as it is less attenuated by light. The best discrimination subset of wavelength was identified using the stepwise discriminant function analysis to determine the best discriminant wavebands to identify *P. oceanica.* These wavelengths are as follows: 328 nm, 408nm, 448nm, 482nm, and 606nm. Major reflectance features were identified in these wavebands. The stepwise discriminant function revealed that spectral separation of the seafloor types is possible with as few as 5 wavebands. The results demonstrate the ability of spectral reflectance characteristics, determined *in situ* the two seafloor types.

Furthermore, to determine whether, *P. oceanica* remains spectrally distinct a Water Colour Simulator (WASI) model was used to simulate *P. oceanica* measurement under adverse conditions. These adverse conditions depth of 4 m, 9m, and 20m and CDOM concentration of 0.010 - 0.10m^{-1}. The WASI model was able to simulate the *P. oceanica* spectra under these adverse conditions. The wavelengths at which they are distinct in adverse conditions were 445, and 485 nm.

The remote sensing of *P. oceanica* is applicable given that the sensor has the bands which are essential for the discrimination of *P. oceanica* from other seafloor types. The MERIS sensor has proven to be a feasible sensor that could be used to map *P. oceanica* as the best discriminant bands identified correlates with the spectral bands of the sensor. However, there are factors that need to be considered in doing so to attain the best results for the managing and the monitoring of this important ecosystem.

Acknowledgements

Praise to the most gracious and merciful, who gave His guidance, will and strength to successfully accomplish my study at ITC.

First of all I would like to express my gratitude to my first supervisor Drs. Valentyn Venus. Thanks for inspiring discussion during research preparation, great and instructive field work and insightful comments during thesis writing; and my co-supervisor Dr. Martin Schlerf and Dr. Bert Toxopeus, for valuable suggestions, scientific and critical comments to improve this thesis project. Indeed I owe both of you for shaping this work and for your encouraging words. I would like to extend my acknowledgements to Syarif Budhiman who assisted me in time of need. I extend my appreciation to all of you and I am grateful to you all.

I would also like to extend my gratitude to Dr. Andy Banks and Dr. Eugenia Apotolaksi for their corporation and advice during field work, and for having us at the Hellenic Centre for Marine Research to use the facilities at the Remote Sensing Laboratory. Dr Magoulas Antonios, Head of Institute of Oceanography at Hellenic Centre for marine Research, who invited us to share the views and importance of this study. The staff members at the Institute of Aquaculture, I appreciate all the facilities offered to carry put my laboratory Experiment. Thanks to staff at the University of Crete for providing us with resources to carry out data collection in the field.

I would like to acknowledge the Erasmus Mundus Lot 10 fellowship programme and University of Belize for giving me this great opportunity to study in the Netherlands. I would like also to give an appreciation to Dr. Michael Weir and Ms. Ceciel Wolters and all ITC-NRM staffs who gave me a good academic atmosphere to learn many new things and to widen my knowledge on GIS and RS subject. I would show my outmost gratitude to Student Affairs office who took very good care of us and our finances.

My sincere gratitude goes to my undergraduate lecturers, Dr. Leandra Ricketts, Dr. Aaron Paul Lewis and Dr. Louis Zabaneh who always encourage me to continue my study and for their invaluable support during scholarships preparations, Dr. Leandra Ricketts, my undergraduate supervisor and lecturer at University of Belize, who open my eyes on the importance of Coastal Zone Marine Studies Thanks to all of you for recommending me to pursue my study at ITC-Netherlands.

I'm grateful to all my cluster-mates for their true friendship and sharing their knowledge and experience for 18 months, my fieldwork-mate: Daniel Louhenapessy, I hope we could fieldwork together somewhere in the world, my other Indonesians friends All others whom I cannot mention one by one, thank you for being my new family in Enschede.

Finally, my deepest gratitude goes to my lovely mom, Alice Noralez for her endless support, immense patience and enormous strength that she gave me during the completion of my study in Enschede. Thank you for being my mom and always motivated me to pursue my never ending dreams. To my father Luther Noralez, who has provided and given me the best education and planting the spirit of courageous. And for Noralez family, with their indefinite and eternal support, thank you, I dedicate this work to all of you.

Table of contents

1. Introduction 7
1.1. Background 7
1.2. *Posidonia oceanica* 7
1.3. Threats to *P. oceanica* Seagrass 8
1.4. Hyperspectral Remote Sensing of Seagrass Ecosystems 8
1.5. Research Problem 9
1.6. Research Objectives: 10
1.6.1. Main Objective: 10
1.6.2. Specific objectives: 10
1.7. Research Question: 10
1.8. Hypothesis: 10
2. Literature Review 11
2.1. Hyperspectral Sensors 12
2.2. Airborne Imaging Spectrometers 12
2.3. Forthcoming Spaceborne Hyperspectral Sensors 13
2.4. Spectroradiometers 13
2.5 Hyperspectral Remote Sensing Applications 14
2.5.1. Hyperspectral Remote Sensing of Shallow Water Habitats 14
3. Methods and Materials 17
3.1. Study Area 17
3.2. Research Scheme 18
3.3. Data Collection 20
3.4. Data Processing 23
3.5. Data Analysis 23
3.6. Spectral Simulation 26
4. Results 31
4.1. Spectroradiometric measurements of Seafloor Types 31
4.2. Underwater Spectral Signatures 32
4.2.1 Posidonia oceanica 32
4.2.2. Carbonate Sand 32
4.3. Student t Test 33
4.4. One Way ANOVA Test 35
4.5. Stepwise Discriminant Analysis 35
4.6. Spectral Simulation 36
4.7. Stepwise Discriminant for Spectral simulation 40
5.Discussion 42
Spectral Discrimination of *in situ* spectral measurements 42
5.1. Spectral Description 42
5.2. Spectral Discrimnation Analysis 44
5.3. Remote Sensing of *P. oceanica* using MERIS 45
5. Conclusion 46
6. Recommendation 47
7. References 48
8. Appendices 54

List of figures

Figure 1: Multispectral (below) vs. hyperspectral sampling (above) 11
Figure 2: Images collected in many contiguous spectral bands create a continuous radiance spectrum. 12
Figure 3: Island of Crete, Greece Mediteranean..... 1
Figure 4: The Research Scheme 18
Figure 5: The Flowchart of Methodology for spectral Discrimination of *P. oceanica* 19
Figure 6: TRIOS Ramses Hyperspectral Radiometers: ARC UV-VIS Radiance sensor (left) and ACC Irradiance sensor (right). 1
Figure 7: Seafloor Types of Agia Pelagia: (A) Carbonate Sand (B*) Posidonia oceanica*..... 1
Figure 8: Diagram illustrating the technique used to measure *in situ* measurements in the field and laboratory..... 1
Figure 9: R_{rs} of seagrass underwater measurement at various depths measured by a remote operated vehicle (ROV), equipped with a SPECTRIX sensors. Figure adopted from (Farmer 2005). 29
Figure 10: Mean apparent reflectance spectra of sand and seagrass (*P. oceanica*)..... 1
Figure 11: Graphical illustration of underwater spectral measurement of submerged *P. oceanica* (blue line) adapted from literature (Maltese et. al., 2008) and the average reflectance of submerged *P. oceanica* (green line) at 1.5m depth measured at Agia Pelagia, Crete. 1
Figure 12: Comparison of measurement taken at top of atmosphere (black lines), bottom for water column (gray lines) and measurement taken from Agia Pelagia (blue line). 1
Figure 13: The results of the Student t test (p values) for all spectral bands and the reflectance spectra of sand and seagrass measured in the field. 34
Figure 14: The results of the Student t test (p values) for all spectral bands and the reflectance spectra of sand and seagrass measured at the laboratory. 1
Figure 15: Mean reflectance spectra of seafloor bottoms with selected bands (black lines) for spectral discrimination 35
Figure 16: Simulated Spectra of *P. oceanica* and Carbonate Sand at 35° sun zenith angle 37
Figure 17: Simulated Spectra of *P. oceanica* and Carbonate Sand at 4m depth using 35° sun zenith angle 38
Figure 18: Simulated Spectra of *P. oceanica* and Carbonate Sand at 4m depth using 35° sun zenith angle 39
Figure 19: The parameters involved in the simulated spectra and its minimum and maximum values of reflectance of the seafloor types at 9m depth 40
Figure 20: : Mean reflectance spectra of seafloor bottoms with selected bands for spectral discrimination for adverse conditions at 4m depth (blue lines) and 20 m depth (red lines)..... 41

List of tables

Table 1: Water Quality Parameters adjusted in the model to reflect Mediterranean Sea Conditions ... 27
Table 2: Table of the WASI parameters used in the forward model for simulation *P. oceanica* seagrass and Carbonate Sand ... 30
Table 3: Fisher's linear classification function coefficients ... 36
Table 4: The parameters involved in the simulated spectra and its minimum and maximum values of reflectance of the seafloor types ... 37
Table 5: The parameters involved in the simulated spectra and its minimum and maximum values of reflectance of the seafloor types at 4m depth ... 38
Table 6: The parameters involved in the simulated spectra and its minimum and maximum values of reflectance of the seafloor types at 20m depth ... 39
Table 7: The parameters involved in the simulated spectra and its minimum and maximum values of reflectance of the seafloor types at 9 m depth ... 40
Table 8:Fisher's linear classification function coefficients at 4 m depth ... 41
Table 9: List of wavelength subsets identified by stepwise selection as those wavelengths without redundancy, provided the greatest separability used by Holden and Ledrew (2003) to classify coral reef bottom types including carbonate sand and seagrass. ... 1

1. Introduction

1.1. Background

Seagrasses are a unique group of submerged aquatic plants that are a vital component of marine ecosystems. They have adapted to exist and thrive in shallow oceanic and estuarine waters throughout the world. They form dense beds –meadows, that are highly productive systems that cover about 0.1 to 0.2% of the global oceans (Duarte, 2002) forming either mono-specific or mixed species meadows with pioneer species such as the *Caulerpa prolifera* , small phanerogams of the genera *Cymodecea* and *Zostera*.

Seagrass ecosystems have been identified as valuable both economically and ecologically. Seagrasses act as the foundation of diverse community with numerous ecological roles: primary production, habitat for other species of plants and animals, food for micro, meso, mega herbivores (including turtles and dugongs), sediment stabilization, biochemical modification of the their local environment and hydrodynamic modifiers. Additionally, seagrass ecosystem provide high-value ecosystem services globally in excess of US$3.8 trillion annually (Costanza et al., 1997). As a result, in comparison to other marine and terrestrial habitats, seagrass meadows play a key role in both ecological functions and are of high economic importance.

1.2. *Posidonia oceanica*

Posidonia oceanica, the dominant and endemic seagrass species in the Mediterranean Sea, extends from 0.4 to 50 meters depth in clear waters covering approximately 2% of the seafloor (Gobert et al., 2006). *P. oceanica* forms monospecific meadows with different types of coverage patterns (continuous to patchy distributions) with shoot densities from very sparse beds (300 m^{-2}) to very dense beds (>700 m^{-2})(Giraud, 1977) forming long-lasting meadows dated back to more than four thousand years old (Mateo et al., 1997). However, because of their sparse sexual reproduction and it requires preferably coarse grain sand and centuries to colonize coastal areas (Duarte, 1995; Kendrick et al., 2005) making it the slowest growing seagrass species (Marba and Duarte, 1998).

Additionally, the shoots of the posidonia plants are borne by rhizomes which grow vertically to avoid burial, or horizontal which enables colonization. These leaves act as sediment traps accumulating organic and inorganic particulate matter (Duarte, 2002). The two types of rhizome growth forms a terraced formation called a “matte” is produced. These “matted” beds can live for 4 -30 years if left undisturbed providing high biomass and high productivity (Hemminga, 2000) growing within oligotrophic or ultra oligotrophic conditions. Eventhough, *P. oceanica* appears to be a minor food source (Dauby, 1989) these leaves support high herbivore production due to its large primary production (J. Cebrián et al., 1999) which are fed upon by fishes and echinoids and turtles. Turtles also spend about 90% of their time at the shallow depths in the vicinity of the meadow and ingest seagrass (Hays et al., 2002). However it is believe that grazing accounts for only a small amount since they contain phenolic compounds (Agostini et al., 2003) which discourages grazing to some consumers. However they are high in biodiversity as the provide shelter, support, breeding and nursing grounds to a wide variety of vertebrates and invertebrates. In addition as sediment trappers they maintain water quality and clarity (Hemminga, 2000).

1.3. Threats to *P. oceanica* Seagrass

Despite the ecological and economical importance of seagrass beds, an increasing number of reports documents the ongoing loss or regression of seagrasses in both tropical and temperate regions throughout the world (Duarte, 2002; Kendrick et al., 2002; Pasqualini et al., 1999; Short and Wyllie-Echeverria, 1996; Waycott et al., 2009). Consequently, rapid seagrass losses over relatively short temporal scales are occurring throughout the world, in places such as the European Mediterranean (Marba et al., 2005), Southern China (Yang and Yang, 2009), Chesapeake Bay (R. J. Orth, 2006), Florida Bay (Fourqurean and Robblee, 1999) in North America and Australia (Dekker et al., 2005; Kendrick et al., 2000; Ralph et al., 2007).

The surface which is covered by *P. oceanica* beds are limited by environmental factors such as light, turbidity, salinity and temperature but in some coastal regions anthropogenic pressures such as trawling, aquaculture, wastewater pollution are having a negative effect causing severe damage and reduction in the both the abundance and distribution of this seagrass species. Recent mapping of Posidonia show declines in seagrass coverage (Kendrick et al., 2000; Pasqualini et al., 1999) which reflects anthropic activities, port developments, grazer impacts, shading of seagrass leaves by excessive growth of epiphytic algae or phytoplankton following nutrient enrichment of waters (Freeman et al., 2008; Short and Wyllie-Echeverria, 1996). Climate change is of concern, as it too will affect seagrass distribution including *P. oceanica*. Accordingly to protect this species, it was nominated as a priority species that required protection to reduce the decline or total loss of this species.

The Mediterranean Sea is considered for its considerable diversity of its fauna and flora as well as for the high rate of species endemism. However, the coastline of Mediterranean countries are intensively used for tourism and related recreational activities, which also have an impact on the quality and clarity of water, which in effect reduces the light reaching the meadow causing mortality which increases the ongoing loss of the species.

1.4. Hyperspectral Remote Sensing of Seagrass Ecosystems

Hyperspectral remote sensing has significantly improved the retrieval of quantitative and qualitative information from vegetation. It has provided the spectral resolution needed to detect reflectance and/or differences in the pigment contents of plants. The ‘hyper’ in hyperspectral refers to the many light sensors with a very narrow sensitive range. The resulting data often has over 100 contiguous bands, each 10 nm or less wide. The high number of bands and the narrow sensitive range enables the detection of changes in the narrow absorption features which may be undetected by broadband sensors. Thus, it has become a solution for surveying the extent and the development of *P. oceanica* and other macrophyte meadows in the Mediterranean Sea. Unlike the optical remote sensing of terrestrial vegetation they are various factors that needs to be considered for proper application to submerged aquatic environments/plants: (1) seagrass and related seabed habitats must be detectable by the remote sensor and (2) the spectral signature from the vegetation must be different from that of surrounding sediments and overlying water.

Seagrasses are covered by a water column that attenuates light reaching, or interacts with the reflectance from the benthos. While the remote sensing of terrestrial plants make significant use of the red edge, aquatic plants such as seagrass cannot be recognized by this feature since

the wavelength beyond 680nm are significantly attenuated by pure water beyond the depth of 1 – 3 m. As a result, the remote sensing of aquatic environments require sensor with greater sensor signal to noise ratio than those used within the terrestrial environments since the absolute reflectance from submerged environments are generally low.

Submerged vegetation like seagrass meadows have been spatially mapped and monitored in many studies using aerial photography such as(Agostini et al., 2003; Kendrick et al., 2000; Leriche et al., 2006; Pasqualini et al., 1999), whereas studies with the use of satellite remote sensing for other submerged aquatic features such as kelp beds (Simms et al., 2001) and coral reefs (Mumby et al., 2004) has proved successful. Nevertheless satellite imagery for mapping seagrass meadows has been successful in clear water of temperate systems (Baden et al., 2003) as well as tropical regions (Phinn et al., 2008; Wabnitz et al., 2008). However the lack of spectral signatures of submerged vegetation measured *in situ* and the uncertainties in water column attenuation has its limitations when using classification algorithms.

1.5. Research Problem

As a result, it is a protected species under the Natura2000 network within the European Union; There is mounting evidence that *Posidonia oceanica*, with an estimated cover of about 50,000 km^2 in the Mediterranean (Bethoux and Copin-Montegut, 1986) has been suffering widespread decline especially in the north west Mediterranean (Marba et al., 1996; Pasqualini et al., 1998). *P. oceanica*, the key species forming meadow communities is responsible for high diversity which provide important functions (Hemminga, 2000) in the Mediterranean. These functions are in jeopardy towards substantial decline of these ecosystems at rates of about 5% yr^{-1} (Marba et al., 2005) faster than the 2% yr^{-2} global rate of decline of seagrass ecosystem (Duarte et al., 2008). Therefore, there is great concern that the functions performed in the Mediterranean will be reduced or lost altogether. Hence, coastal management strategies and seagrass conservation programs have evidenced the importance of *P. oceanica* mapping to monitor the changes in their distribution.

Monitoring of marine benthic communities is an essential activity to increase the understanding of change in marine habitats and ensure the best management of ecosystems within coastal areas. The conventional methods such as field mapping and aerial photography are time consuming and expensive, and they lack either sensitivity or quantitative information. Additionally, traditional remote sensing instruments do not have the spatial or spectral resolution to readily distinguish different benthic types. Hence, the capabilities of new airborne instruments provided potential, as well as the driving force for the development of qualitative hyperspectral measurements and model-based methods for mapping seagrass and associated ecosystems.

With developments in recent years of satellite remote sensing, high resolution sensing data has been used to detect the living status and distribution of *Posidonia oceanica* seagrass. (Pasqualini et al., 2005) used SPOT 5 data to map the distribution of *Posidonia oceanica* along Zakynthos Island in Greece with Principle Component Analysis. (Fornes et al., 2006) applied IKNOS data to detect *Posidonia oceanica* in the Mediterranean Sea and found that seagrass beds distributed 15m underwater can be detected clearly. (Vela et al., 2008) used fused images of SPOT 5 and IKONOS to assess the distribution of seagrass meadows in lagoons and other regional countries of the Mediterranean Sea. (Piazzi et al., 2000) was able to integrate indirect and direct methods to map

Posidonia oceanica in western Mediterranean islands. Eventhough, research has found that broadband and hyperspectral imagery can detect benthic environments, the mention under which condition they are mapped are yet to be explored. Hence this study will explore whether *Posidonia oceanica* beds can be mapped at certain depths given that it remains distinct under varying conditions. The result of this study can assist in identifying spectral bands that are able to discriminate *P. oceanica* form other seafloor types.

1.6. Research Objectives:

1.6.1. Main Objective:

Study seagrass and seagrass characteristics and uncertainties associated with signal-to-noise due to radiometric distortion inherent to remote sensing of sub-merged vegetation.

1.6.2. Specific objectives:

1. Discriminate between *Posidonia oceanica* and other seafloor cover types based on narrow-band spectral observations.
2.

1.7. Research Question:

1. Is *Posidonia oceanica* spectrally distinct from other seafloor cover types?

1.8. Hypothesis:

1.1.1 H_0: There is no statistical significant difference ($p \leq 0.05$) between the spectral signature of *Posidonia oceanica* and other seafloor cover types.

$\mu_1 = \mu_2 = \mu_3$

Ha_1: There is a statistical significant difference ($p \geq 0.05$) between the spectral signature of *Posidonia oceanica* and other seafloor cover types.

$\mu_1 \neq \mu_2 \neq \mu_3$

2. Literature Review

The use of remotely sensed data in cover type discrimination has evolved coral reef features delineation and relatively successful within group classification using broadband and multispectral type sensors. However, using higher spectral resolution sensors has proven to be more accurate in classifying coral reef ecosystems. Spectral resolution is perhaps the most important property of sensors used for this application as they have to be able to resolve that natural variability in the system being studied. Broadband sensors cannot resolve fine diagnostic spectral features, as their spectral bandwidths are 100 – 200nm and are not contiguous (Holden and LeDrew, 1998; Vane and Goetz, 1988). Hyperspectral data was thought to be well suited for this application, as it is by definition, consist of a set of contiguous bands and usually stretches across a relatively wide wavelength range (Goetz, 2009). The difference between the spectral resolutions for multispectral and hyperspectral is very evident in Figure 1.

For spectral separability of submerged aquatic vegetation, for example coral reef features, a hyperspectral spectrometer would have to record a spectrum from 400 nm – 700 nm; this spectral range is of primary importance for oceanographic communities, with a resolution of 10nm or less and have a signal-to-noise ratio smaller than the depth of the absorption feature of interest (Curran, 1994). Two types of hyperspectral sensors: airborne imaging spectrometers and ground based spectroradiometers will be discussed followed by a discussion of the application of hyperspectral data in shallow reef environments and its use for determining spectral separability of coral reef features.

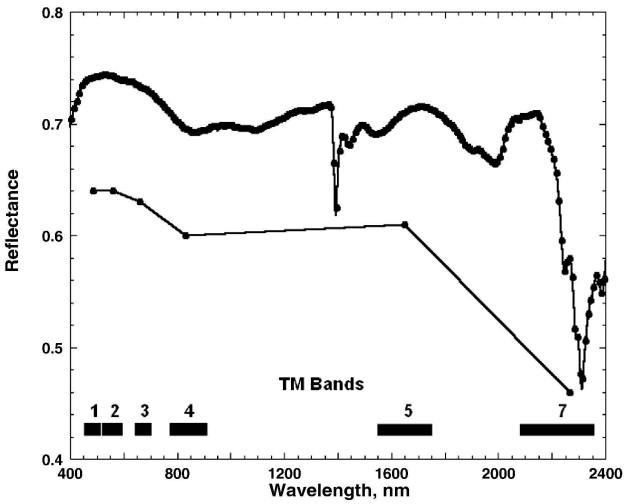

Figure 1: Multispectral (below) vs. hyperspectral sampling (above)

2.1. Hyperspectral Sensors

The first types of sensors to be discussed are the airborne imaging spectrometers. These sensors provide a radiance (digital number) reading for each picture element (varying in size) for a set of contiguous wavebands at high (±10nm bandwidths) spectral resolution. An example of this sensor application can be seen in Figure 2. As of yet there is not a spaceborne hyperspectral sensor available, so only airborne sensors will be discussed at this time. The second type of sensors is the spectroradiometers, which are usually ground based. Data are also collected in a contiguous fashion, using a foreoptic with a specified viewing angle. Thus reflectance values for the target for all the bands are gathered and stored as numerical values, which can be represented as a reflectance graph.

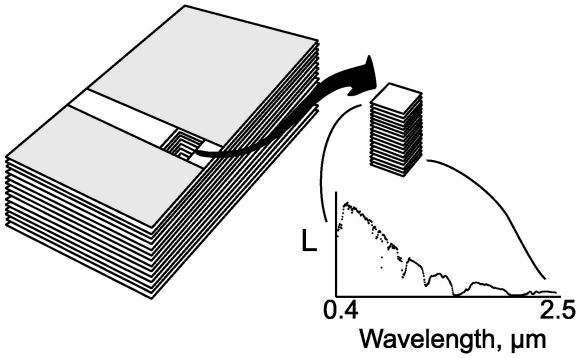

Figure 2: Images collected in many contiguous spectral bands create a continuous radiance spectrum.

2.2. Airborne Imaging Spectrometers

The first imaging spectrometer to measure solar reflected spectrum form 400 nm to 2500 nm at 10nm intervals was the AVRIS sensor from NASA's Jet Propulsion Laboratories, which became operational in 1987. Radiance spectra are collected as images of 11 km width and up to 800 km in length. AVRIS acquires its data from NASA ER-2 aircraft at an altitude of 2000 m(Green et al., 1998). The preceding sensor was called AIS (Airborne Imaging Spectrometer), and the last version had a spectral coverage ranging from 800 – 2400 nm. The AIS sensor had fairly low signal-to-noise (40:1 up to 110:1) as well as other problems such as vertical stripping after radiometric calibration (Vane and Goetz, 1988). AVRIS on the other hand, boast a very high signal-to-noise (exceeding 100:1 requirement) especially after improvements were made to the sensor in 1995 (Vane and Goetz, 1988). Hyperspectral sensors that have followed include HYDICE, CASI, DAIS (2815 and 7915) MVIS, TRWS-III and Hymap /Probe 1 (Birk and McCord, 1994). Nineteen different airborne hyperspectral system and 14 agencies with data acquisition aircraft were in existence in 1994(Birk and McCord, 1994). Since then there have been updated and changes made to these sensor and new one s have been developed since. The characteristics of sensors vary from sensor to sensor, but the set of properties that define hyperspectral sensors namely: a broad spectral range, contiguous bands and high spectral

resolution, remain the same. CASI, for instance offers imaging capabilities in 288 contiguous spectral bands ranging from 430 – 870, with an average spectral resolution of 3nm.(Lewotsky, 1994).

2.3. Forthcoming Spaceborne Hyperspectral Sensors

Only airborne hyperspectral sensors are currently for both commercial and government use. The trend of remote sensing platforms moving away from large complex civil governmental and military systems to an increasing number of purely commercial, hybrid governmental/commercial and commercial/university collaboration systems is changing the face of remote sensing industry. As the application and implications of remote sensing data for commercial ventures become more evident, the sensors are evolving to meet new needs and better address old ones. Just as spatial resolution has dropped to 1 meter and below for commercially available imagery, spectral resolution's importance and applications are also becoming to the fore(Glackin, 1998).

(Glackin, 1998) predicts that the number of spectral bands in space based electro-optical systems will increase dramatically from 1998 – 2007. Multispectral imagery will most probably have as many as 36 bands (MODIS instrument), while hyperspectral spaceborne sensors like these to be aboard OrbView-4 and the Naval EarthMap Observer (NEMO) are to be launched within this frame. The OrbView-4 Hyperspectral Imager (HSI) for example, will have 200 hyperspectral channels (450 – 2500nm) at 8 m spatial resolution and a swath of 5km. The same instrument will also have 4 m, 4 channels) and panchromatic (1m, 1 channel) capabilities, making it extremely versatile by extending its application milieu tremendously (Glackin, 1998).

With commercial hyperspectral sensors such as these becoming available in the future, the necessity for research to establish hyperspectral data's niche is even more important. Old problems could be addressed using new technologies and algorithms, and the user's ability to solve new problems that may arise becomes much better.

2.4. Spectroradiometers

Spectroradiometers can be both imaging and non-imaging. In this study, reference is made to non imaging spectrometer. Spectroradiometers have been used with varying success for different applications. These instruments are usually ground based and can be used in laboratory or in-field conditions depending on the make and the model. In this case, objects are pre-identified and there spectral responses are recorded for comparative purposes or for correlation between or within objects/targets under observation. A large number of laboratory and field based studies have been undertaken to investigate the feasibility of utilising high spectral data for vegetation studies such as leaf biochemical and biophysical components(Cho et al., 2007; Ferwerda, 2005; Skidmore et al., 2005), quantity and quality of terrestrial vegetation(Ferwerda, 2005; Skidmore et al., 2005) , species discrimination base on spectral differences(Sobhan, 2007), and species distribution in saltmarshes (Schmidt, 2003).

2.5 Hyperspectral Remote Sensing Applications

For much of the past decade, hyperspectral imaging and its applications has been an area of active research and development. Many features on the earth's surface can be identified by unique absorption features in their reflectance spectra. The knowledge has been used in attempts to identify features (or feature groups) from remote sensing platforms and in doing subsequent classification of imagery. Hyperspectral Imaging and non imaging applications have found to be valuable and beneficial in resource management, agriculture, mineral exploration and environmental monitoring. For example, hyperspectral remote sensing in agricultural is becoming actively important in precision farming (Pacheco et al., 2008) as hyperspectral data is being as valuable in assessing crop and soil conditions which has increasingly contributed to the economic value in agricultural production. Additionally, in forestry applications hyperspectral data has been used utilized in many forest areas, viz., forest planning and management, forest inventory, forest area monitoring (Kamaruzaman and Kasawani, 2009), and water resources (Gitelson and Merzlyak, 1996; McWire et al., 2000; Underwood et al., 2003) for assessing water quality(Shafique et al., 2001), flood detection and monitoring(Felipe et al., 2006).

In this study, hyperspectral remote sensing of benthic habits and the studies concerning the separability and/or discrimination of these features will be discussed. The remote sensing of shallow water environments and the discrimination based on the spectral differences between and within groups (i.e. seafloor types) will be further discussed.

2.5.1. Hyperspectral Remote Sensing of Shallow Water Habitats

Most hyperspectral studies within shallow water habitats pertain to submersed features of coral reef habitat mapping. Eventhough case studies applying remote sensing to benthic habitat mapping have been constrained by sensor capabilities, sensor systems have not been specifically tailored to submersed features or feature groups. Additionally, the water column is of major concern for applying remote sensing techniques. In contrast to the remote sensing of terrestrial vegetation, there is practically no signal returning from the water or the substrate at wavelengths beyond 680 nm due to the absorption by pure water (Platt, 1995). Recent developments and new techniques have enabled the improvement of the accuracy for mapping and monitoring of these resources. Good reviews of the history and current status of coral remote sensing has been done by various researchers(Green et al., 1996). These review notes that most research has been evaluated with data provided by multispectral scanners, airborne multi and hyperspectral imaging system.

Historically, aerial photography and navigational charts have been the basis of knowledge for the geographical extent of benthic habitats such as coral reefs. However, navigational charts are restricted to deep areas accessible by ship-borne depth sounders and photographic coverage of these benthic assemblages are often out of date due to the expenses involved in acquiring such images. Aerial photographs, on the other hand, are unlikely to have ground verification performed at the time of the capture. This could be a source of error, thus reducing the overall precision limiting the interpretability and geo-positional accuracy of the photographs. Hence

remote sensing offers an excellent option and is of primary use among researchers and mangers for consistent, repetitive monitoring of shallow water habitats for both large and remote areas.

Remote sensing techniques have been applied to study benthic habitats, especially coral reefs, around the world. Due to the current technological limitations, the testing of different sensors for benthic habitat is of great interest to researchers of different fields. For instance, (Malthus and Mumby, 2003) evaluated three optical remote sensing methods for measuring standing crop in the tropical Western Atalntic. Empirical relationships of field data with imagery from Landsat Thematic mapper, SPOT and CASI data to predict standing crop was defined. The benefits and monitoring considerations were also discussed.

As it is known, remote sensing has been used to analyse terrestrial features within the visible and infrared range of the electromagnetic spectrum, to study soil mineral content, foliage density and type, and surface elevation (Clark, 1993; Curran, 1994) using both satellite and airborne sensors. However, the sensors are more limited when used over oceans or lakes because of the low reflectance values of deep water (giving relative low signal-to-noise ratios) due to the complexities of combined water and bottom signals in shallow waters(Jerlov, 1976). In other words, a significant problem involved with the remote sensing of submerged ecosystems is the water column overlying the substrate significantly affects the remotely sensed signal due to the optical attenuation of light in water (Andréfouët et al., 2001; Green et al., 1996; Holden and LeDrew, 2001; Mobley, 1994) in addition to light scattered in the atmosphere (path radiance).

Optical properties of benthic substrates are of great concern when using remote sensing techniques to study benthic habitats. Spectral reflectance of coral species have been analysed and well studied. (Hochberg et al., 2003) collected *in situ* spectral reflectance of three coral species, five algal species, and three sand benthic communities in Kaneohe bay in Oahu in Hawaii. They identified major reflectance features and applied linear discriminant functions to an AAHIS (Advance Airborne Hyperspectral Imaging System) image.

(Holden and LeDrew, 2001) took *in situ* reflectance measurements of corals in the U.S. Virgin Islands at various depths over different substratum. They made a comparison between hyperspectral reflectance measured at the top and bottom of the water column in different water depths. Hyperspectral discrimination of healthy versus stressed corals in Fiji Islands, South Pacific, St. Croiux, and U.S. Virgin Islands and developed a high spectral resolution library. (Hochberg et al., 2003) measured 13,100 *in situ* optical reflectance spectra of 12 reef bottom types in Atlantic, Pacific and Indian Oceans. The fundamental bottom types were classified, spectra processed and the spectral separability of bottom types using a classification analysis following a partition method (Lehmann, 1998; Rencher, 1995).

The scientific community is presently evaluating different sensors to study coastal areas. (Hochberg et al., 2003) assess the capabilities of seven remote sensors to classify coral, algae and carbonate sand as pure and mixed spectra based on 10,632 reflectance spectra measured *in situ* around the world reefs. They studied the spectral response of two hyperspectral sensors, AAHIS and AVIRIS, and three satellite multispectral sensors, IKONOS, Landsat ETM and SPOT- HRV, and two future satellite narrowband multispectral sensors, PROTO and CRESPO. They conducted discriminant, classification and spectral mixing analysis, and image simulation. Results based on linearly mixed-sensor specific spectra demonstrate that the hyperspectral and

narrowband multispectral sensors discriminate between coral and algae across many levels of mixing, while broadband sensors do not. However, narrowband sensors overestimate coral cover. They conclude that it is necessary to design a sensor system specialized to coastal studies. (Andrefouet and Robinson, 2003) assessed the potential of IKONOS data for coral reef habitat mapping. Ten IKONOS images of reef habitats around the world were processed, including correction of sea surface roughness and bathymetry, supervised and unsupervised classifications, and accuracy assessment based on ground truth data. The results of IKONOS classification were compared with Landsat 7 data for simple to moderate complexity of reef habitats. Results showed a general linear trend of decreasing accuracy with increasing habitat complexity. In general, IKONOS performed better in accuracy compared to Landsat. The applied sea surface correction (Hochberg et al., 2003) uses the near infrared band to characterize the spatial distribution of relative glint intensity, which is scaled by absolute glint intensity in the visible bands. The result is subtracted from the visible bands filtering out glint effects. Mumby and Edwards (2002) compared satellite and airborne systems to define habitat categories, supervise image classification, and make an independent assessment of thematic map accuracy. They used CASI, IKONOS, TM, MSS, and SPOT-HVR data.

2.5.2 Water Column Distortions and Spectral Simulation

The subsurface irradiance and remote sensing reflectance, R and R_{rs} are wavelength dependent functions of absorption a (λ) and backscattering b (λ), and strongly influenced by substances suspended and dissolved in water. Additionally, in shallow water areas, the detected signal is affected by light reflected at the bottom. The influence of water constituents and bottom affects optical signal at some spectral regions (Albert and Gege, 2006) making it difficult to distinguish each effect and its interactions with the target under observation and thus reducing the accuracy of quantitative data from remote sensing techniques used for mapping benthic substrates.

As a solution, forward models were developed based on radiative transfer in water where the reflected signal is calculated as a function of optical properties of water and the water constituents. Thus raditiative transfer models allow the modelling of radiation as it travels through the atmosphere and water column. Included in the modelling processes is the overlying water column, thus allowing the reflectance of substrates to be predicted over a range of water depths (Holden and LeDrew, 2002; Kutser et al., 2003) using a physics based model known as Hydrolight by Curtis D. Mobley. Researchers has found it useful to study light field under varying condition of optical properties by measuring and determining model parameters from a measured spectrum, for example, the concentration of water constituents, bottom depth, and bottom characteristics like submersed vegetation for mapping and monitoring water quality parameters (Brando and Dekker, 2003) and benthic substrates (Richardson et al., 2006).

3. Methods and Materials

3.1. Study Area

Crete is one of the 13 regions into which Greece is divided. Crete Island is the largest of the Greek Islands and the fifth largest island in the Mediterranean. The geographic coordinates of Crete lies from 23°31' to 26°18'E and 34°55' to 35°41N which has an elongated shape that covers 8, 336 km² which spans 260 km from east to west and 60 km at its widest points. The total length of Crete's coastline is 1046 km consisting of both sandy beaches and rocky shores. Administratively Crete is divided into four nomos or prefectures namely: Chania, Rethymno, Lasithi and Heraklion which is inhabited by 650,000 inhabitants (Garvey, 2007).

Crete is extremely mountainous and is defined by a high mountain range crossing from West to East formed by three different groups of mountains (i.e. Leftka Ori (2452m); The Idi Range :Mt Psiloritis (2456m); the Dikti Mountains (2148m)). Crete Island straddles two climatic zones, the Mediterranean climate and the North African climate with mild winters and hot summers (temperatures above 40°C). The atmosphere is quite humid, depending on the proximity to the sea. Snowfall is common in the mountains between November and May, but rare and low in the coastal areas. The South coast is an exception, which includes the Messara plain and Asterousia Mountains, which fall in the North African Climate zone and therefore enjoys significantly more sunny days and high temperatures throughout the year.

Figure 3: Island of Crete, Greece Mediteranean

Heraklion is the largest city in Crete and is the fourth largest city in Crete. The Prefecture of Heraklion lies in the central eastern part of Crete. It borders the Prefectures of Lasithi to the east and Rethymno to the west, abutting the Cretan sea in the north and the Libyan Sea in the south. Heraklion covers 2, 641 km. This prefecture is mostly plain and semi mountainous and it is one of the most populated prefectures with 26 municipalities, 194 municipal districts and 460 villages. This Municipality is inhabited by 292, 482 situated in the valleys of farmlands both in the central and northern parts and the coastlines of the prefecture.

3.2. Research Scheme

Figure 3 summarizes the steps followed for the investigation of spectral discrimination of *P. oceanica* seagrass. Whereas, Figure 4 illustrates the flowchart of the specific steps taken throughout the paper to answer the objective of the study.

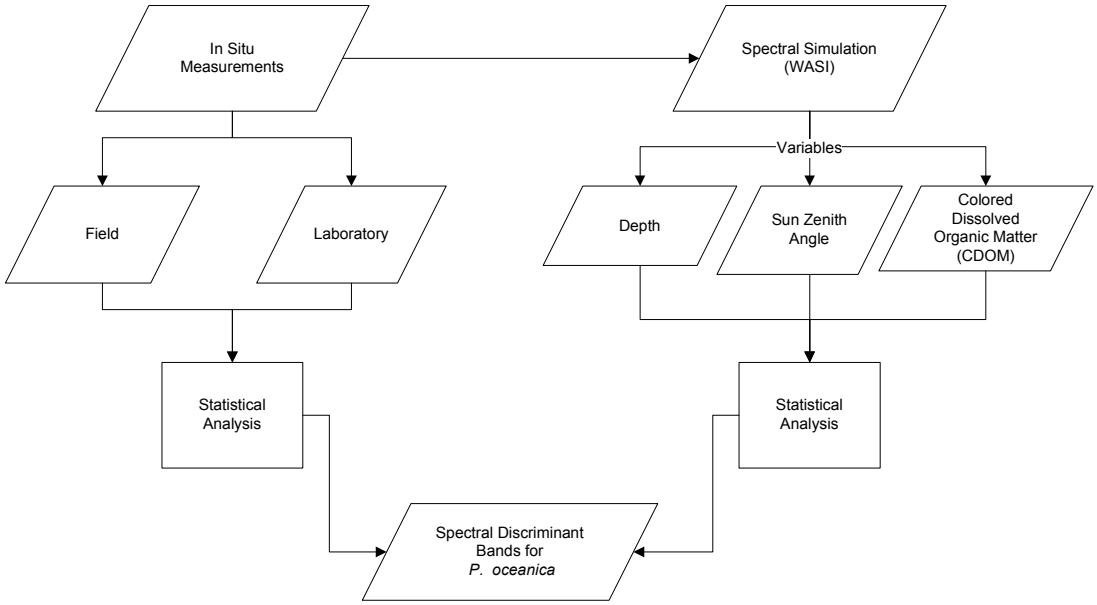

Figure 4: The Research Scheme

Agia Pelagia is a village lying on the northern coast of Crete, 20 km north-west of Heraklion. It has long white sandy beaches and is a touristic coastal town. The reason why the field data collection was conducted in this area is because the bay is protected from wave-creating north winds and the sea state is almost always serene. The areas had sparse seagrass beds not more and within shallow areas ranging from 0 – 1.5 m, which was within reach for measurements to be taken.

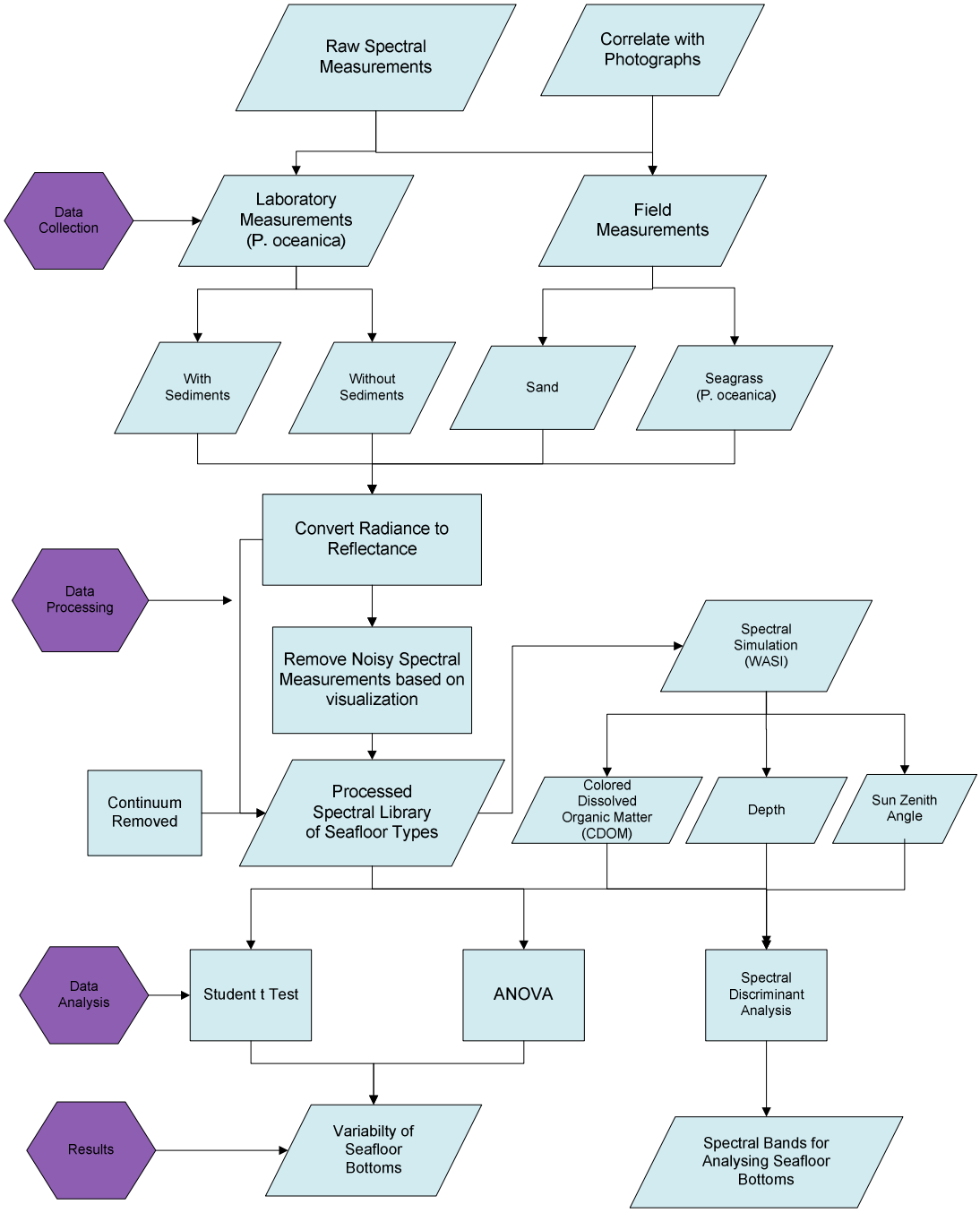

Figure 5: The Flowchart of Methodology for spectral Discrimination of *P. oceanica*

3.3. Data Collection

Fieldwork was conducted from September 28th to October 18th 2009. September 28th to October 14th, field data collection was conducted. Photographs of the seafloor was taken to determine the presence and absence of seagrass within the NATURA 2000 Network which would be used to compare the mapping accuracy of seagrass meadows at various sites namely Sitia, Xerokampus and Frankastello. The 15th to 16th October; laboratory data collection was carried out at the Cretaquaruim where seagrass was measured under variable conditions: with sediments and without sediments.

3.3.1. Field *in situ* Measurements

Underwater *in situ* spectral measurements of different benthic assemblages were collected with a TRIOS Ramses ARC sensor seen in Figure 3. The spectrometer collected light in the wavelength range 320 – 950 nm, with an optical resolution of 5 nm. The sensor had a 7 degree field of view and was held at a distance of 20 cm from the target of interest, to sample a radius of approximately 8.7 cm. Sample sites chosen hosted two benthic types in water depth of 1.5 m. Datasets of spectral signatures was derived for two benthic types in Figure 4.

Figure 6: TRIOS Ramses Hyperspectral Radiometers: ARC UV-VIS Radiance sensor (left) and ACC Irradiance sensor (right).

Spectral measurements were taken on sunny, cloud free day; the sea state during data collection was fortunately calm. The spectrometer was programmed to take automatic measurements in burst mode, where measurements are taken as fast as possible. Additionally with this setting, if the device receives any data the measurement is taken immediately. The sensor head was held underwater using a platform and the sampling was controlled by an operator on the surface boat. The head of the sensor was pointed downward at an angle of 0 (nadir view) degrees to the desired specimen to capture the spatial variability in the radiance for the benthic substrates. The frame had a 45 degree angle to maintain the sensor looking down at 0 degree (nadir view). An underwater camera was attached to the platform to assist with the identification of the target being measured. An illustration of the setup was made clear in the diagram below Figure 8.

The radiance data was converted from an analogue to digital signal and transferred via a power cable to a laptop on the boat. Simultaneously, a reference panel was used to estimate the incident downwelling irradiance (E_d (λ)), at the same depth and distance from target to enable the determination of percent reflectance.

Figure 7: Seafloor Types of Agia Pelagia: (A) Carbonate Sand (B*) Posidonia oceanica*

One discrepancy of this sampling design that had to be resolved was the area on the bottom of the instantaneous field of view (IFOV) of the sensor was different depending on the height of the sensor. When immersing the sensor in the water they were varying depths at which measurement were taken, however when the sensor was held at 20cm above substrate at the bottom of the water column the radius of the measurement was 8.7cm. The radius was calculated using equation 1. Additionally, there was an offset of the camera on the platform due to the distance of the sensor from the platform as seen in Figure 8. Thus, the photographs did not correlate with the type of substrate being measured at that specific time.

$$Raduis \equiv d \times \tan\left(\frac{FOV}{2}\right) \qquad (1)$$

Where d is the distance or height above the bottom substrate and the FOV is the field of view of the sensor (7°). The area measured at the bottom of the water column was therefore consistent for all measurements since the height above the bottom remained consistent.

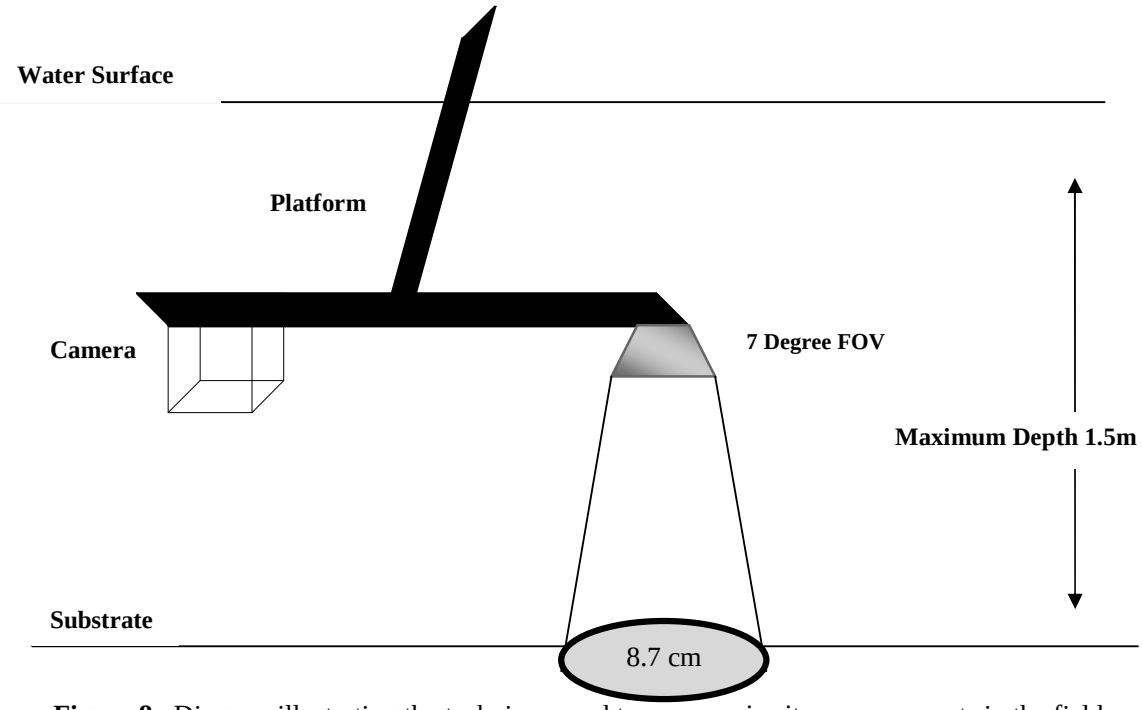

Figure 8: Diagram illustrating the technique used to measure *in situ* measurements in the field and laboratory

3.3.2 Seagrass Sampling

To measure seagrass under variable conditions in controlled conditions, seagrass sampling was performed. Seagrass and sediments were collected from Agia Pelagia. To maintain the homogeneity of the seagrass samples seagrass and sediments were collected from the same site. Sampling was performed by a volunteer diver.

Seagrass was collected from the edges of the meadow to avoid destruction of the seagrass meadow. A knife was used to carefully retrieve the seagrass including the leaves, stem, rhizome and roots. Approximately 200 shoots were collected to perform the laboratory experiment. Dark plastic containers filled with seawater were used for storing the seagrass shoots to avoid any desiccation or stressed to samples and maintain suitable conditions during the travel from site to laboratory.

3.3.3 Laboratory *in situ* Measurements

To study the influence of suspended sediments when acquiring spectral measurements of seagrass a laboratory experiment was conducted. Laboratory spectral measurements were conducted at the Hellenic Centre for Marine Research (HCMR) at the Institute of Aquaculture (Appendix 1,). Two land based aquariums were allocated for the laboratory test to be conducted. They were 1.5 m depth and holds up 2000 gallons of seawater. The aquarium was equipped with oxygen to extend the longevity of the plants for the 2 days they would be in the tank.

As aforementioned, two tanks were set up to study seagrass under two different conditions: (1) Without sediments and (2) With sediments. Aquarium 1 (without sediments) was prepared for measurement. Seagrass was rinsed with clean water to remove any sediment. Clean seagrass with rhizomes and roots were place the plastic grid to hold the seagrass in place. Approximately 100 shoots were used for each measurement to make an 8.7 cm field of view (FOV) required for measuring the seagrass. Strings were used to hold the grids in the aquarium. In Aquarium 2 (with sediments) sediments were introduced. Seagrass were placed in plastic containers with the sediments collected from the site in Agia Pelagia and weighed down by pebbles. The water was slightly stirred to suspend the sediments and measurements were taken.

3.4. Data Processing

Data of the spectral measurements taken in field and at the laboratory were processed. The field *in situ* and the laboratory data was converted from radiance to reflectance. Reflectance was then calculated as the ratio of spectral upwelling radiance to downwelling irradiance at a given wavelength (Mobley 1994). This assumed that both panels and benthic surfaces reflected equally in all directions (i.e. (Lambertian reflectors) :

$$R \equiv \frac{L_u(\lambda)}{E_d(\lambda)} \qquad (2)$$

Noisy spectra were removed based on visual inspection. Aquarium measurements of seagrass were compared to field measurements of seagrass since the pictures taken in the field was not able to match with the field measurements. The spectral reflectance from individual features measured was edited from 318 to 818 nm to work with the visible spectrum range. The spectral shapes were visually inspected for recognition of discriminant patterns and identification of wavelength location of peaks. An average of 10 spectral reflectance of each feature was calculated to reduce the variance between replicates and facilitate the creation of a spectral library. Two spectral libraries were created using spectral tools on ENVI. They are the spectral reflectance of field measurements and laboratory measurements.

3.5. Data Analysis

An exploratory data analysis was performed to check the variability and distribution within each waveband for each variable: sand, seagrass, seagrass without sediments and seagrass with sediments. All data were tested for normality computing the Kolmogorov- Smirnov and the Shapiro Statistic to determine the right test to apply: parametric or non- parametric.

Statistical test was used to compare between the spectral responses of the 2 individual seafloor types. This was performed to determine whether the pair of them was statistically different at every spectral band. Student's T test was performed for field measurements and Analysis of Variance (ANOVA) for both laboratory and field measurements were performed. Discriminant Analysis was also performed to determine the variability and the spectral separability of these features. Discriminant function analysis was used to determine which variables discriminate between two or more naturally occurring groups. Box plots and tables were created to help

visualize the data. The tables and box plot indicated that separation between the seafloor types, however further investigation into the statistical significance was necessary.

3.5.1 Student's T Test

Student's T test (t test) for independent samples is a parametric test used to compare two means collected independently from one another. It is one of the most commonly used techniques for testing a hypothesis on the difference between sample means. Simply stated, the t test determines the probability that two populations are the same with respect to the variable tested; the variable, in this case, the wavebands of electromagnetic spectrum. Thus, the spectral responses of field measurements: seagrass and sand; and laboratory measurements: seagrass without sediments and seagrass with sediments were tested using the t test to identify the spectral differences within each waveband between groups are "significant". Hence the student's t test was found to be appropriate and was used to compare the means of the two seafloor types measured in the field and laboratory. This aim was addressed testing the following null hypothesis:

$$H_o: \mu_1 = \mu_2 \tag{3}$$

$$H_o: \mu_3 = \mu_4 \tag{4}$$

Where μ_1 is seafloor type 1, *P. oceanica*; μ_2 is seafloor type 2, sand; μ_3 laboratory experiment without treatment 1, *P. oceanica* without sand; μ_4 is laboratory experiment with treatment *P. oceanica* with sand.

In testing the null hypothesis to determine whether the population mean within wavebands are equal for laboratory and field measurements, the statistic below was used:

$$t \equiv \frac{x - \mu_0}{\sqrt{n}} \tag{5}$$

Where *s* is the standard deviation of the sample and *n* is the sample size. The degree of freedom used in this test is *n-1*.

3.5.2 One Way Analysis of Variance (ANOVA)

One way analysis of variance was performed to compare between the spectral responses of both laboratory and field measurements. The aim of the ANOVA test was mainly to visualize statistically the spectral differences between the laboratory and field measurements. The test was chosen because direct visualization is not an effective tool for comparing all measurements. In other words, the spectral variations within an individual species (intra-species spectral

variations) cause spectral overlaps which makes it difficult to identify the spectral differences between groups (inter-species spectral variation) with the naked eye. The application of ANOVA test assisted to highlight poor locations at which p values were greater than α (α = 0.05, α =0.01). Whereas, p values higher than α at some locations will indicate whether the spectra of the seafloor types were very similar as none of them was statistically separable from the groups. On the other hand, the p values less than the α threshold will indicate that there is statistical significance. The ANOVA test is therefore a rapid way to visualize the spectral differences by demonstrating that spectral separability responses of seafloor types is likely at certain spectral positions. The research hypothesis that the means of reflectance between the seafloor types in the field and the laboratory were statistically significant at each measured waveband was test viz the null hypothesis (6) versus the alternative hypothesis (7):

$$H_o: \mu_1 = \mu_2 = \mu_3 = \mu_4 \quad (6)$$

$$H_a: \mu \neq_1 \neq \mu_2 \neq \mu_3 \neq \mu_4 \quad (7)$$

Where μ_1 is the mean reflectance values of *P. oceanica*, and μ_2, μ_3, μ_4, are the mean reflectance values from sand, P. oceanic without sediments, and *P. oceanica* with sediments respectively.

In testing the null hypothesis to determine whether the mean spectral responses within wavebands are equal for laboratory and field measurements, the F statistic was used.

Finally a Tukey HSD multiple comparison test was performed to determine which means are significantly different to other from other means.

3.5.3 Stepwise Discriminant Analysis

Discriminant analysis is a technique used to build a predictive linear model of group membership based on observed characteristics of each case. First, it proceed by testing for differences among the dependable variable or groups; second, if the test supports the alternative hypothesis of significant among groups, the analysis proceeds to find the Fisher's linear combinations (called discriminant functions) of the independent variables that best discriminate among groups. It generates function from samples of cases for which group membership is known.

To determine the spectral separability of bottom types, canonical stepwise discriminant analysis was performed in the SPSS software using the standardized discriminant and the unstandardized identification functions, for both spectral libraries of seafloor bottoms. The canonical variables were plotted for the spectral separability to show where separability occurs between different groups.

A stepwise discriminant analysis was performed on the datasets to identify the variables that would maximise differences between the statistical groups (between seafloor types) while minimising within group differences at the same time. Stepwise analysis means that statistical criteria alone determine the order of entry of variable, depending on how much each variable explains the variance. Therefore, Stepwise Discriminant Analysis (SDA) is a selection method that repeats the addition and removal of a feature at each step. This process allows us to find the best subset with which satisfactory discriminatory or separability can be obtained. Furthermore, a multivariate discriminant procedure was performed using the variables shown by the stepwise discriminant procedure to be significant for distinguishing between statistical groups. The coefficients are used to assess the contributions of the wavelength to the final discrimination.

The stepwise procedure is 'guided' by the respective *F* to enter and F to remove values. The *F* value for the variable indicates the statistical significance by the separability or the discrimination between groups. In this study, the Wilk's Lambda to determine the significance of separability between the bands for the two targets measured.

Wilk's Lamda (λ)

Wilk's lamda is a multivariate test. It ranges between 0 and 1. Values that are close to 0 indicate the group means are different, values close to 1 indicates that the group means are not different and thus the alternative hypothesis could not be rejected.

Finding the Important regions

After selecting bands by using the above discrimination procedures, results were pooled in a frequency plot. The bands were grouped to form spectral region with maximum frequency of occurrence based on distribution and frequency of occurrence.

3.6. Spectral Simulation

Several water constituents influence water colour. These optically active components include suspended matter, phytoplankton, and the different absorbing pigments, detritus and coloured dissolved organic matter (CDOM) called Gelbstoff. The mentioned components scatter and absorb light in a different spectral manner resulting in a non linear relationship between their concentrations and the reflectance of water.

To further asses the spectral discrimination of *P. oceanica,* the Water Colour Simulator (WASI) model was used to simulate spectra varying various parameters listed in Table 1. The WASI is a sensor- independent spectra generator and spectra analyzer with well documented calculation steps and automatic result visualization. Forward and inverse calculation for the spectrum types at a range of at least 390 – 800nm with a 1nm spectral resolution can be simulated and analyzed using this model. The data provided with the model was determined at Lake Constance (*Boddensee*) (Gege, 2004; Heege and Fischer, 2004), a freshwater lake which borders Germany and Switzerland. The model was set for marine environment and water quality

parameters were adjusted to better reflect the Mediterranean water conditions. The water parameters are as follows: concentration of Chlorophyll a, concentration of small particles.

The parameters and ranges are listed in the **table 2** below.

Water Parameter	Description	Ranges
$\mathbf{C_i}$	Concentration of Phytoplankton Class	0.035 -0.089 ug $^{-l}$
$\mathbf{C_s}$	Concentration of small particles	< 5 mg l^{-1}
n	Exponent of Backscattering by small particles	0.005 m^2g^{-1}
T	Water temperature	17-25 ℃
Y	Concentration of Gelbstoff	0.010 - 0.100
Constants		**Default Value**
$\boldsymbol{\lambda_O}$	Reference Wavelength for Gelbstoff absorption	440
$\boldsymbol{\lambda_S}$	Reference wavelength for scattering of small particles	500
$\mathbf{b_1}$	Backscattering coefficient of saline waters	0.00144 m $^{-1}$
$\mathbf{b_{bS}}$	Specific backscattering for small particles	0.005 m^2g^{-1}
$\mathbf{K_0}$	Coefficient of Attentuation	1.0546
$\mathbf{B_n}$	BDRF of bottom reflectance (sand)	0.318 sr $^{-1}$

Table 1: Water Quality Parameters adjusted in the model to reflect Mediterranean Sea Conditions

For this study, forward calculations were simulated for remote sensing reflectance (R_{rs}) in shallow water were simulated to determine if *P. oceanica* is spectral distinct under the different alterations of various parameters. The variability of a spectrum is determined by up to 25 parameters, which could be seen in Appendix 2. The three parameters altered for this study were: depth, Gelbstoff/CDOM, and sun zenith angle. These parameters are important to the simulation of the spectra of *P. oceanica* as the alterations will determine the accuracy in mapping the submerged vegetation(Duarte et al., 2007; Foden et al., 2008; Kelble et al., 2005; Kendrick et al., 2005; Vahtmae et al., 2006).

Optical properties of water have a major contribution to the reflectance of the bottom type that captured by the satellite or airborne sensor. Depth, Gelbstoff and Sun angle are important factors that determine when, how and what will be capture by the sensor when the conditions are appropriate. In shallow water, the optical properties are very complex in comparison to that of deep water (Mobley, 1994). Hence the depth at which *P. oceanica* could be captured by a sensor is important to know as these plant species are regressing and needs to be monitored to be conserved. CDOM is a major absorber of light in water and the concentration within water will determine the amount of light that should be available for plants to photosynthesise.

3.6.1 Parameters

Coloured Dissolved Organic Matter

The biological and optical characteristics of coastal and estuarine waters are complicated by temporal and spatial variability in the concentrations of coloured dissolved organic matter (CDOM) and suspended particulate matter (SPM), the spectral properties of pure water, and the composition of phytoplankton photosynthetic pigments. The variability of CDOM concentration in coastal waters is influenced by the terrestrial input, primarily composed of humic acids produced from decomposition of plant litter and organically rich soils within coastal watersheds and upland areas.

One indicator of health in estuarine and coastal environments is the ability to transmit sunlight to planktonic, macrophytic and other submerged vegetation for photosynthesis. The concentration CDOM (Gelbstoff) is a primary factor affecting the absorption on incident sunlight in coastal and estuarine waters. At increasing level of concentrations, CDOM absorption could affect primary productivity and ecosystem structure by reducing the amount and quality of photosynthetically active radiation (PAR) to phytoplankton. Additionally, CDOM is the major ultraviolet light (UBA and UVB; 280- 320 and 320-400 nm respectively) absorber within most if the global ocean surface (Morel et al., 2007) and a significant fraction of the visible light (400 – 700 nm) the marine environments (Allali et al., 1995; Silio-Calzada et al., 2008), thus depressing the water-leaving radiance recorded by the remote sensors.(English and Carder, 2005).

P. oceanica is well adapted to eutrpohic waters than that of oligotrophic zone. (Alcoverro, 2001) determined the photosynthetic capacity of *P. oceanica* in two contrasting nutrient zone and found that the photosynthetic capacity was two times higher in the relatively eutrpohic zones. In eutrophic zones, light is the dominant regulator and there is a coherent patter between light and photosynthetic capacities. Thus, it could be said that light is the primary factor influencing photosynthesis and depth distribution of submerged plant (Duarte, 1991) such as *P. oceanica* for growth and survival. Since CDOM is a major absorber of light, how does the variation in the simulation affect the remote sensing reflectance of seagrass and its ability to be mapped. The range of CDOM concentration for the Mediterranean is known to be 0.0100 – 0.100 m^{-1} (Siegel, 2005). This range will be used to understand the effect of CDOM concentration will be varied to imitate eutropthic environment using ranges adopted from Mobley"s L*ight and Water*, and thus determine at what concentration of CDOM is *P. oceanica* spectrally distinct

Depth

The seagrass depth range refers to the maximum depth that seagrass could be found. Duarte examined the depth limits of seagrass of many species and showed that seagrass may extend from a mean sea level down to a depth of 90 m (Duarte, 1991). The differences in the depth limit (zB) are largely attributed to the light attenuation (K) underwater due to suspended solids, chlorophyll a and dissolved organic matter. When depth increases, light penetration decreases because the irradiance within sunlit and sky lit water decreases exponentially with depth. The light transmitted through water and its constituents further modify light entering the water through processes of absorption and scattering before reaching the plant canopy (Larkum et al., 2006; Maritorena et al., 1994). However this is dependent on the transparency and clarity of

water and the concentration of constituents in the water. Once again, this depresses the water leaving radiance received by the sensor. The figure below demonstrates that as depth increases the remote sensing reflectance decreases (Scott, 2005). Hence the alteration of depth in the WASI model will assist in determining at what depths P. oceanica could be captured to be mapped using a airborne or satellite sensor.

P. oceanica maximum depth range is approximately at 45 m. It is known that at depth greater than 4 m waters are significant attenuation by scattering and absorption by water constituents further restricts light passing to and reflecting back from the benthos (Dekker, 2002). Could the pigmented related spectral features of *P. oceanica* within the visible wavelengths be distinct from other seafloor beds at depths greater than 4 m? In the model the depth parameter was varied from 5, 10, and 15 - 20 m to approve or disprove that *P. oceanica* is spectrally distinct in deep waters. A spectral discriminant analysis is done using the simulations to determine which wavebands can be used to identify *P. oceanica*. At an appropriate depth at which the spectral discrimination could still be determined for mapping.

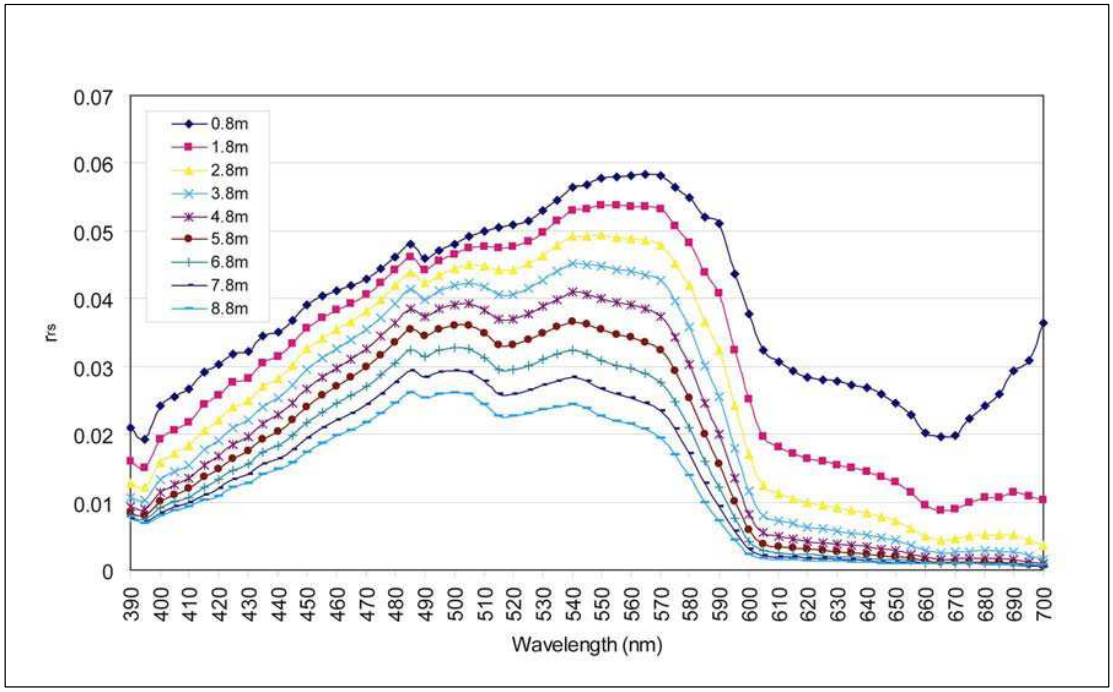

Figure 9: R_{rs} of seagrass underwater measurement at various depths measured by a remote operated vehicle (ROV), equipped with a SPECTRIX sensors. Figure adopted from (Farmer 2005).

Sun Zenith Angle

The computation of R involves radiance in all directions (Mobley, 2004). However, above water remote sensing reflectance of optically shallow waters is done for a limited range of solar zenith angles (Mobley, 2004, Valta-Hulkkonen et. al, 2004) and the BRDF effects on the water leaving radiance, or equivalently on the remote sensing reflectance, for solar angles is relevant to remote sensing.

Bidirectional reflectance distribution function (Martonchick et. al, 2000) describes the reflectance of a target as a function of the viewing and illumination geometries, expressed un terms of four angles: the solar zenith angle, (θ), solar azimuth angle (φ), sensor zenith angle (θ_r) and sensor azimuth angle (φ_r). The magnitude of bidirectional effects depends on the sun target –sensor geometry, wavelength and the physical characteristics of the target. For this study, solar zenith angle will be altered to investigate whether the changes in the sun angle contribute to the differing spectral reflectance behaviour. This will determine the best time of the day at which imaging could be performed.

Table 2: Table of the WASI parameters used in the forward model for simulation *P. oceanica* seagrass and Carbonate Sand

Scenario	Parameter	Ranges
	Depth	4, 9, 20
	CDOM	0.010 - 0.100
	Sun angle	35 -45

4. Results

4.1. Spectroradiometric measurements of Seafloor Types

Clear separation was observed between the mean (+SD) spectral signatures for the seagrass and sand spectral signatures for the samples measured in natural condition; whereas, for laboratory measurements, the spectral measurements are visually similar as can be seen in Figure 10. The reflectance spectra of sand had the highest reflectance values and they show the least variation in the shape Figure 10. The seagrass spectra, on the other hand had lower reflectance value compared to the sand spectra. This is an indication that the bare sediments could be easily separated from the other bottom types on the basis of brightness alone.

Seagrass reflectance spectra displayed a reflectance minimum at approximately 670nm, a feature related to the presence of chlorophyll a + b. This reflectance minimum is exhibited weakly in the sand spectra indicating the presence of benthic micro algae within the substrate. The reflectance of sand and seagrass were distinguishable as they were no overlap of spectral signatures throughout the wavelength.

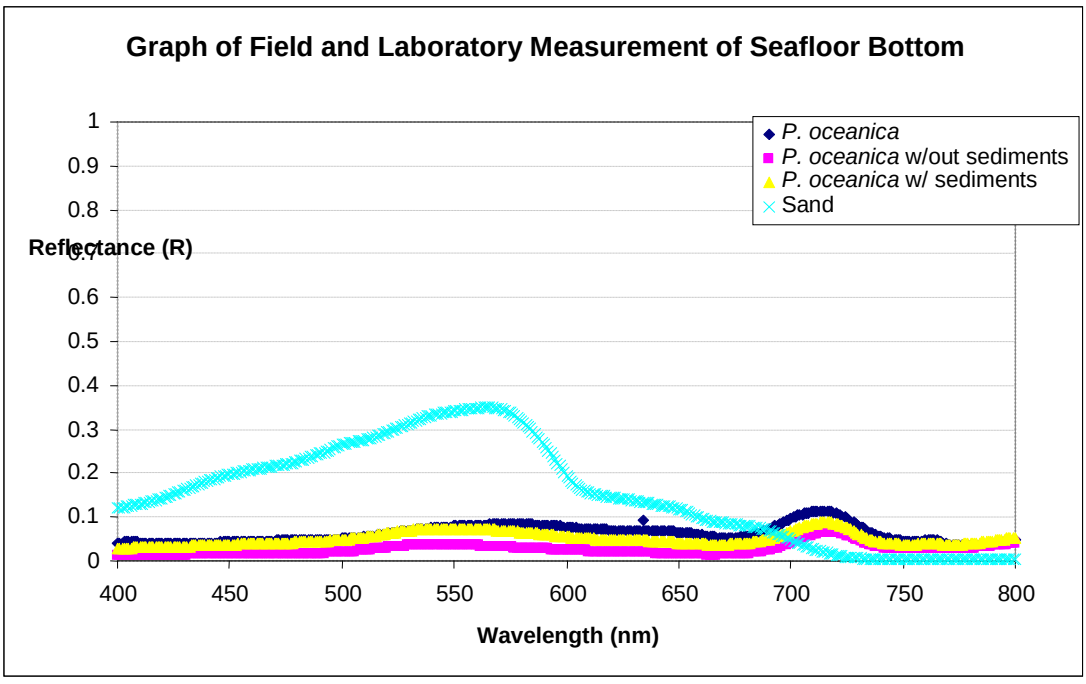

Figure 10: Mean apparent reflectance spectra of sand and seagrass (*P. oceanica*).

4.2. Underwater Spectral Signatures

4.2.1 Posidonia oceanica

The mean of the spectral signature of *Posidonia oceanica* measured underwater are shown in Figure 7. The sorbet absorption features could be observed around 490nm and 668nm, while reflectance peaks were observed at wavelength 525 nm to 618 nm with the centre being at 568nm. *P. oceanica* peaks at the longer wavelengths in the visible regions and the red- edge feature for the *in situ* spectra was lost due to the strong attenuation and very low signal recorded at these wavelengths. Similarities are observed between the *in situ* measurements taken at Agia Pelagia and *in situ* reflectance (Rf) of (Maltese et al., 2008) which was conducted in Stagnone di Marsala Lagoon, on the west coast of Italy in summer of 2007.

Eventhough, the shape of the *in situ* spectra measurements of *P. oceanica* are similar, the reflectance (Rf) of Maltese study is relatively higher than the spectral reflectance of *P. oceanica* for this study. Factors that contributed to the differences in spectral signature of *P. oceanica* will be discussed later.

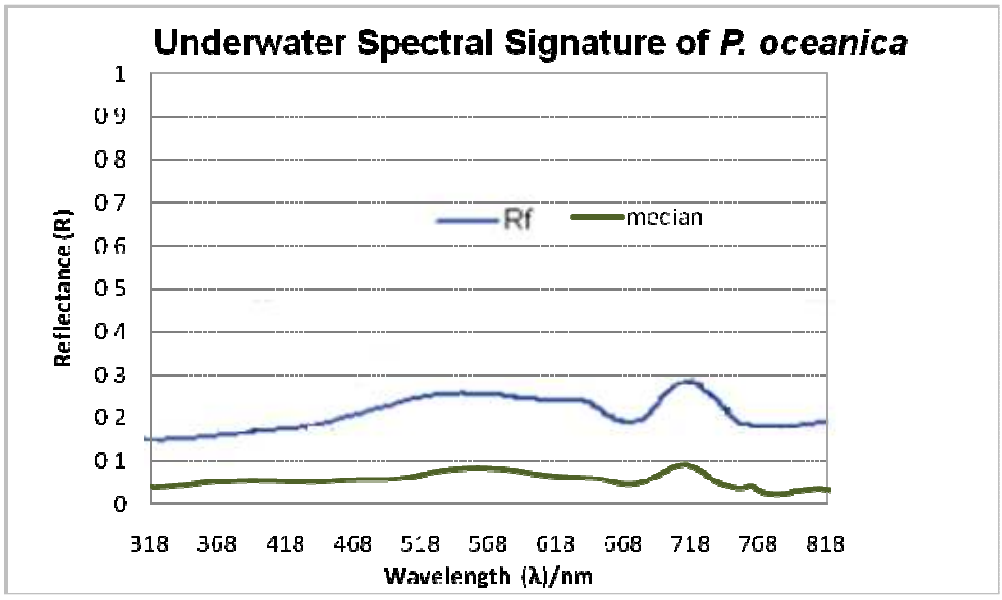

Figure 11: Graphical illustration of underwater spectral measurement of submerged *P. oceanica* (blue line) adapted from literature (Maltese et. al 2008) and the average reflectance of submerged *P. oceanica* (green line) at 1.5m depth measured at Agia Pelagia, Crete.

4.2.2. Carbonate Sand

The mean of the sand spectra was higher than the mean reflectance of *P. oceanica*. The sandy bottoms studied during our field experiments were relatively bright white sand (Maritorena et al., 2004). Thus, the *in situ* measurement of carbonate sand had higher reflectance values in comparison to *P. oceanica*.

In figure 12 below, the sand spectra taken in Agia Pelagia is compared to bottom albedo of sand at the depth of 1.5m done in US Virgin Islands (Holden and LeDrew, 2001). Measurements at

the top-of-water column and underwater were conducted to evaluate the effect of water column on bottom type identification and detection of benthic habitat. Carbonate sand has a very high reflectance, with minimum value of 5% at 350 nm and reaching maximum values of 34% at the highest peaks for both underwater signatures (grey and blue lines in Figure 12) at 570 nm. The factors that influence the spectral signature of underwater environment will be discussed later.

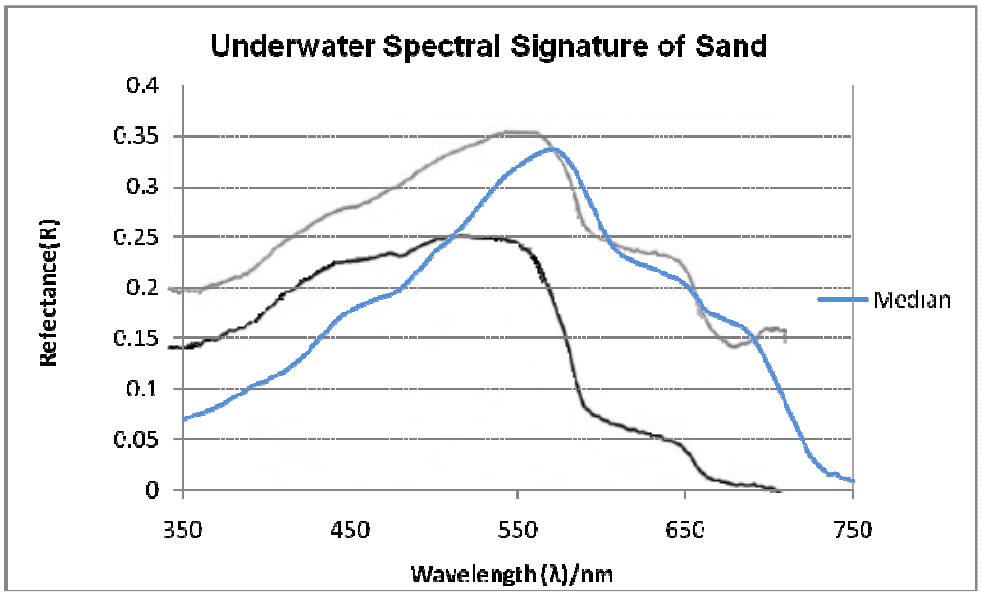

Figure 12: Comparison of measurement taken at top of atmosphere (black lines), bottom for water column (gray lines) and measurement taken from Agia Pelagia (blue line).

4.3. Student t Test

The seafloor types under study were statistically significant at the spectral bands, with a 95% confidence level (p value < 0.05). The results of the Student t test (p values) for all spectral bands were plotted in Figure 9. The reflectance spectra of sand and seagrass measured in the field was also drawn in the figure to show the continuum of both spectral signatures collected by the spectrometer. The total number of spectral bands that had p values less than 0.05 was 162 bands, of which 161 bands had a 99% confidence level (p value < 0. 01). The exceptions were located in the red (696 – 703 nm) and the near infrared region (862- 962 nm) as there were overlaps of both spectral measurements at these regions.

T test was also performed to compare the means of laboratory measurements and laboratory measurements. The t test for *P. oceanica* with sediments versus *P. oceanica* without sediments was performed. The number of spectral bands that had a p value less than 0.05 was 123 bands, whereas 122 of these bands had a 99% confidence level (p value <0.01). The exceptions were once again, located in the red and infrared region of the electromagnetic spectrum. Seagrass with sediments had higher reflectance values than that of seagrass without sediments. We can conclude that the visible region of the spectrum is the least affect by the attenuation of water and most appropriate to use for analysis.

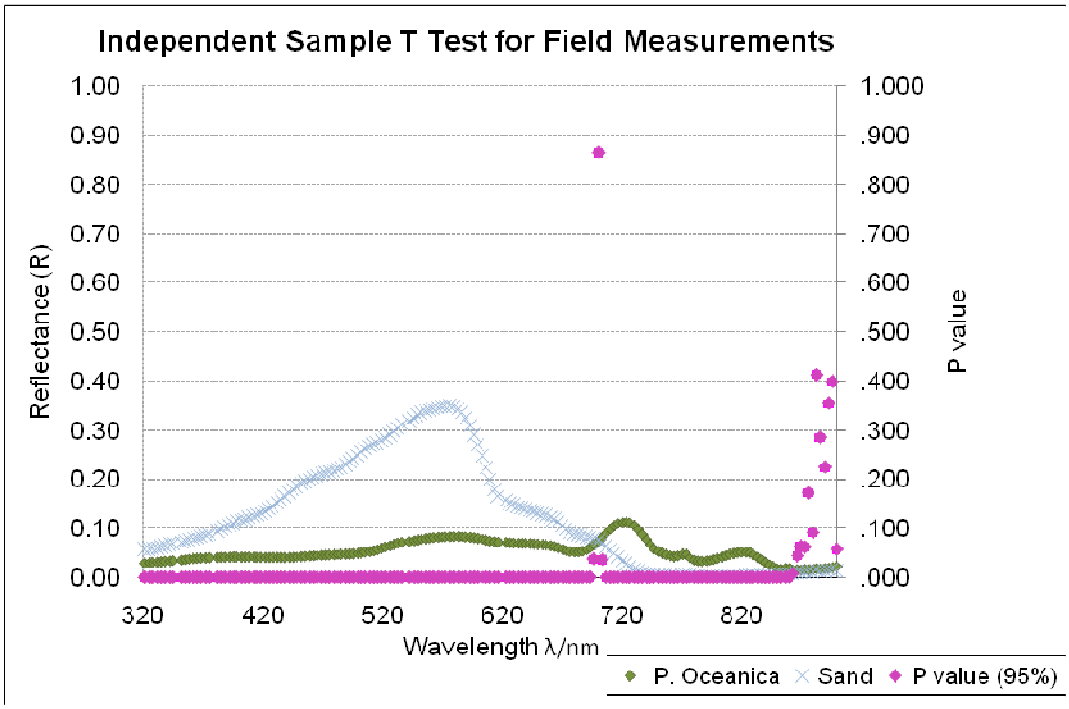

Figure 13: The results of the Student t test (p values) for all spectral bands and the reflectance spectra of sand and seagrass measured in the field.

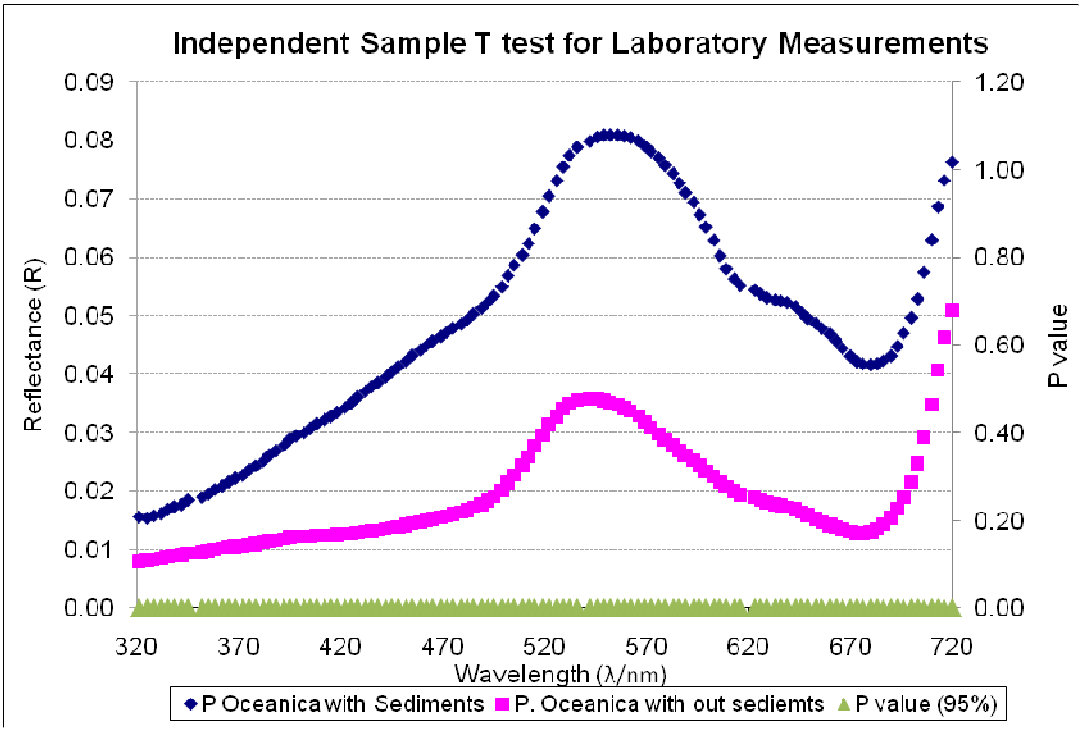

Figure 14: The results of the Student t test (p values) for all spectral bands and the reflectance spectra of sand and seagrass measured at the laboratory.

4.4. One Way ANOVA Test

The result of the 170 ANOVA test (p values) for all spectral bands were plotted in Figure 10. The measured spectra of *P. oceanica* with and without sediments were statistically different at most of the spectral locations, with a 95% confidence level (p value < 0. 05). The F values of the test are greater than F critical value, 2.64 at 0.05 confidence level which clearly indicates that differences between the field and laboratory measurements exists. The Tukey HSD post hoc illustrated statistical difference between pairs measured at different wavebands.

4.5. Stepwise Discriminant Analysis

The multivariate stepwise discriminant analysis of the seafloor types of the spectral library produced a list of wavelengths that better discriminant the variables with a significance of 95%. (See selected bands in Figure 15; see Stepwise statistics in Appendix 3) These selected wavelengths differ significantly between seafloor types.

Selected wavelengths: 328, 408, 448, 482, 606, 736, 786, 856, 952

By visual inspection of the spectral curves, the last 3 wavelengths: 786 nm, 856 nm, 952 nm is not considered valid because it is in the upper range if the NIR region of the spectrum and penetration of light is very low, thus there is a lot of noise distorting the reflectance curves. However, the other wavelengths are known to be within the blue and green regions of the visible spectrum and are the two ranges that are used to study features that are usually submerged by water.

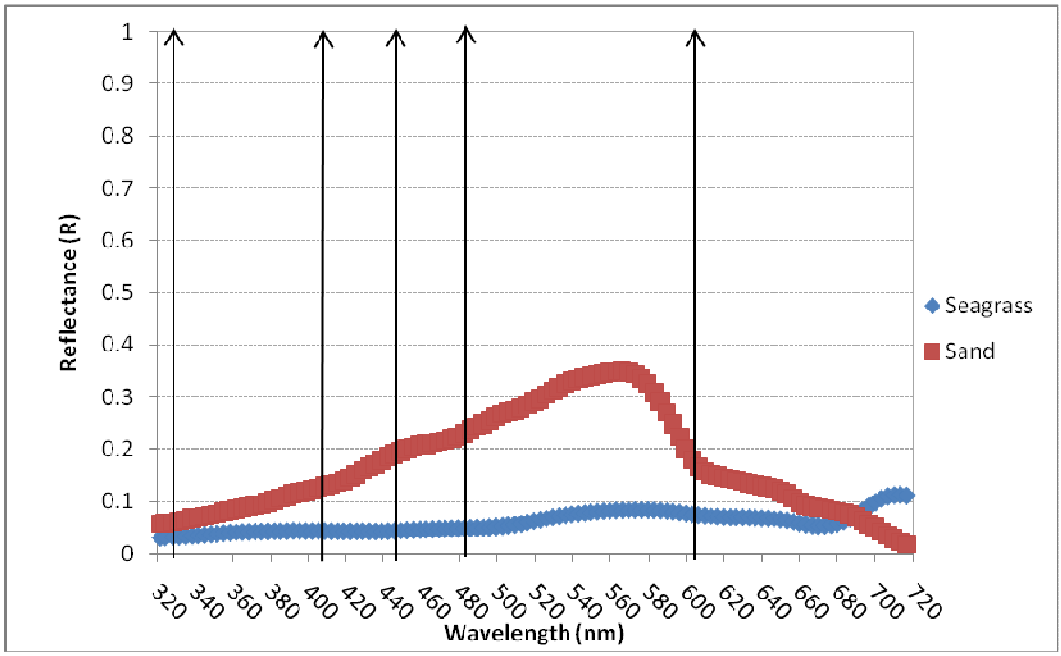

Figure 15: Mean reflectance spectra of seafloor bottoms with selected bands (black lines) for spectral discrimination

The first canonical discriminant function was used in the analysis and 100% of the variance was explained. (See selected bands in Figure 15; see Stepwise statistics in Appendix 3)**.** Fisher's linear classification functions shows that using the only function, wavelength 448 nm shows the highest coefficient (- 553.997) of classification for *P. oceanica* and for sand (3297.553) and to a lesser extent but also important to discriminate are wavelengths 328 nm, 408 nm, 486nm and 606 nm.

Table 3: Fisher's linear classification function coefficients

Wavelength	Seafloor Type	
	Posidonia oceanica	Sand
328	944.060	1864.185
408	-475.468	-2573.043
448	-553.997	3297.553
482	603.255	-1702.271
606	-80.575	103.876

These coefficient are statistically significant as is observed from the Wilk's Lambda, thus we reject he null hypothesis as there is statistically significance between the two seafloor types at a depth of 1.5m. Using these wavelengths, *P. oceanica* can be discriminated from other seafloor types.

4.6. Spectral Simulation

Parameters

The WASI Model simulations for seagrass, *P. oceanica* and carbonate sand were simulated using the scenarios mentioned in Table 2. The following figures below demonstrate visually the differences between two seafloor types.

Difference in reflectance was not apparent immediately when the sun angle was altered. However, from the Figure 15 and Table 2, at 35° Sun zenith angle the reflectance of both seafloor type was at its maximum value of 2.5 % reflectance and as the zenith angle increases at 40 ° and 45° (Appendix 5) there was little variability observed in the reflectance of the seafloor bottoms where reflectance where less than 2%.

Additionally, these reflectance values at these sun zenith angles were due to its interaction with the presence of CDOM or lack thereof. When CDOM values were low the reflectance of seafloor was at its maximum and vice versa. Therefore, the interaction with the said parameter has an influence on the reflectance at the various SZA presented.

The maximum depth range that *P. oceanica* was found to be at 45 m (Duarte, 1991). However, for simulation the maximum depth of 20m depth was choosen as the maximum as the model outputs remain constant after 20m.

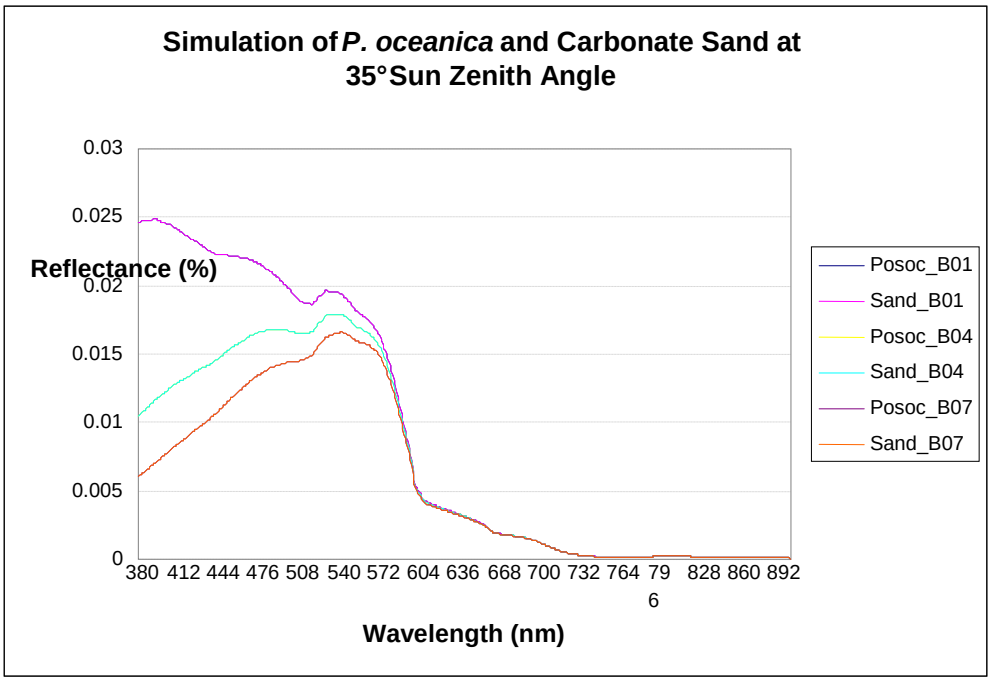

Figure 16: Simulated Spectra of *P. oceanica* and Carbonate Sand at 35° sun zenith angle

Table 4: The parameters involved in the simulated spectra and its minimum and maximum values of reflectance of the seafloor types

	Parameters		*P. oceanica*		Sand	
Spectrum	Gelbstoff (m^{-1})	SZA (°)	Minimum	Maximum	Minimum	Maximum
B01	0.01	35	0.00006189	0.02487	0.00006189	0.02487
B04	0.055	35	0.00006189	0.01795	0.00006189	0.01795
B07	0.1	35	0.00006189	0.0162	0.00006189	0.01662

Even though the sun zenith angle the effect of the sun angle was not visually evident in the reflectance of the seafloor types, when depth was altered the reflectance of the seafloor was adversely affected as *P. oceanica* had lower reflectance value in comparison to carbonate sand.

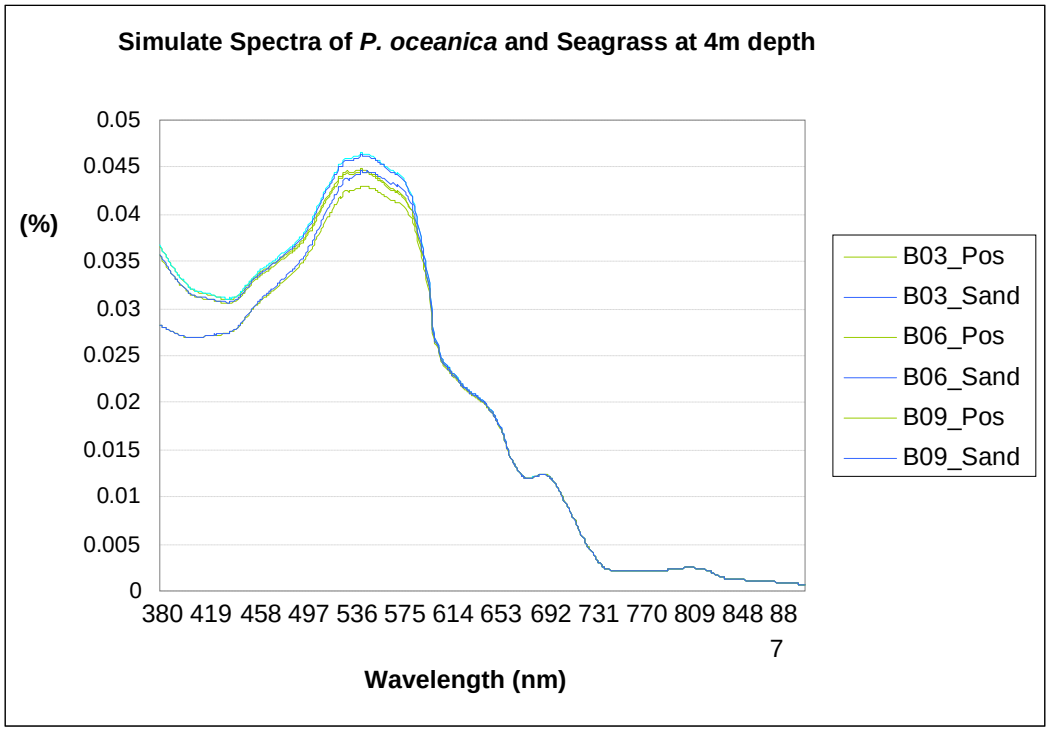

Figure 17: Simulated Spectra of *P. oceanica* and Carbonate Sand at 4m depth using 35° sun zenith angle

Since 35° degree zentih angle was determine the appropriate angle to attain the presumbly good refelctance values for the seafloor types, this SZA was used as a constant. On the other hand, the CDOM range (0.010 -0.10 m^{-1}) remained the same as it was appropriate for conditions representative of the Medetranean Sea. The other SZA is demonstrated in Appendix 5.

Table 5: The parameters involved in the simulated spectra and its minimum and maximum values of reflectance of the seafloor types at 4m depth

	Parameter		*P. oceanica*		Carbonate Sand	
Spectrum	Gelbstoff (m^{-1})	Depth (m)	Minimum	Maximum	Minimum	Maximum
B03	0.01	4	0.000703	0.04485	0.000703	0.04657
B06	0.055	4	0.000703	0.04657	0.000703	0.04637
B09	0.1	4	0.000703	0.04466	0.000703	0.000703

At 4 m depth, reflectance of *P. oceanica* was at its maximum with 4.7 % (Table 4) and continuously decreases to 0.08 % (Table 5) at 20m. The simulated spectra of *P. oceanica* demonstrate that with greater the depths the reflectance value decreases. The variability of reflectance seen in the green region is slightly evident and eventually disappears in the red and near infrared regions as water and it optical properties attenuates light which decreases the light penetration. As result of decreased variability due to the interaction with the optical properties, the simulated spectra overlap to such an extent that spectral discrimination is unlikely.

As can be observed, the simulated spectra of *P. oceanica* at this is masked by the carbonate sand simulated spectra. The influence of the bottom albdeo is apparent in the simulation of the

model and thus overshadows the pigmentation of the plant which is absorbed rather than reflected back to the sensor (Pinnel, 2003). In Appendix 6 where the depth is lower, overlap of spectra is not visible.

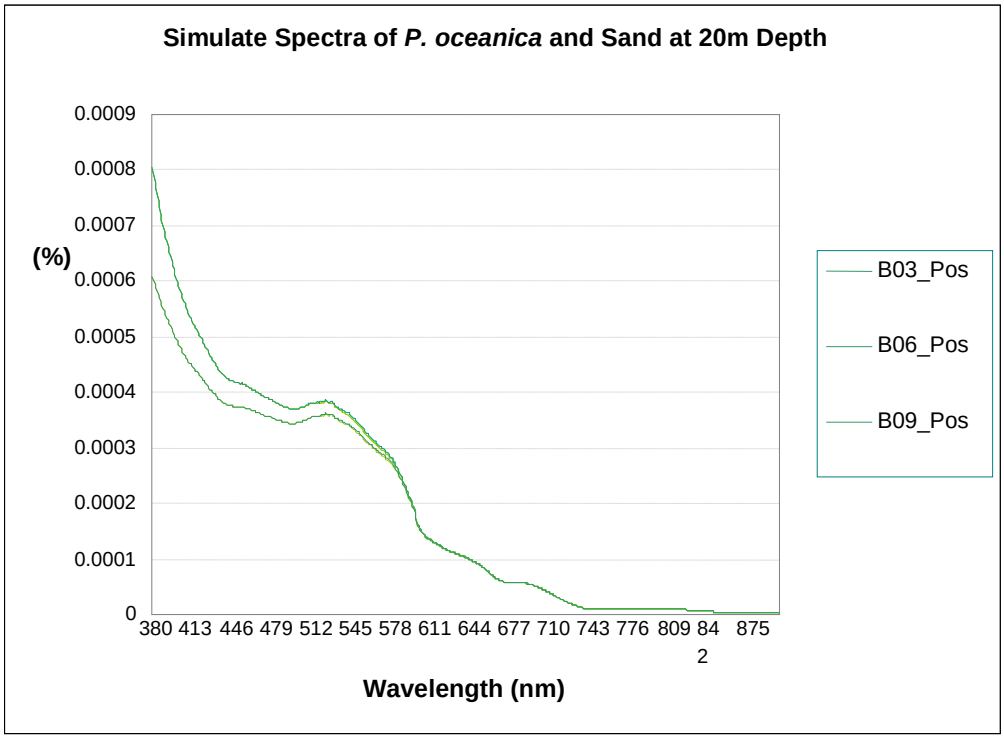

Figure 18: Simulated Spectra of *P. oceanica* and Carbonate Sand at 4m depth using 35° sun zenith angle

On the other hand, at depth of 9m, reflectance values are lower, less than 1% (Table 6) perhaps when compared to the reflectance simulated at 4m. Nevertheless, the variability exhibited from the pigmentation due to chlorophyll content within the angiosperm, is apparent from both seafloor types as seen in Figure 18.

Table 6: The parameters involved in the simulated spectra and its minimum and maximum values of reflectance of the seafloor types at 20m depth

	Parameter		*P. oceanica*		Carbonate Sand	
Spectrum	Gelbstoff (m^{-1})	Depth (m)	Minimum	Maximum	Minimum	Maximum
B03	0.01	20	2.8E-06	0.000804	0.000002797	0.000804
B06	0.055	20	2.8E-06	0.000804	0.000002797	0.000804
B09	0.1	20	2.8E-06	0.000608	0.000002797	0.000608

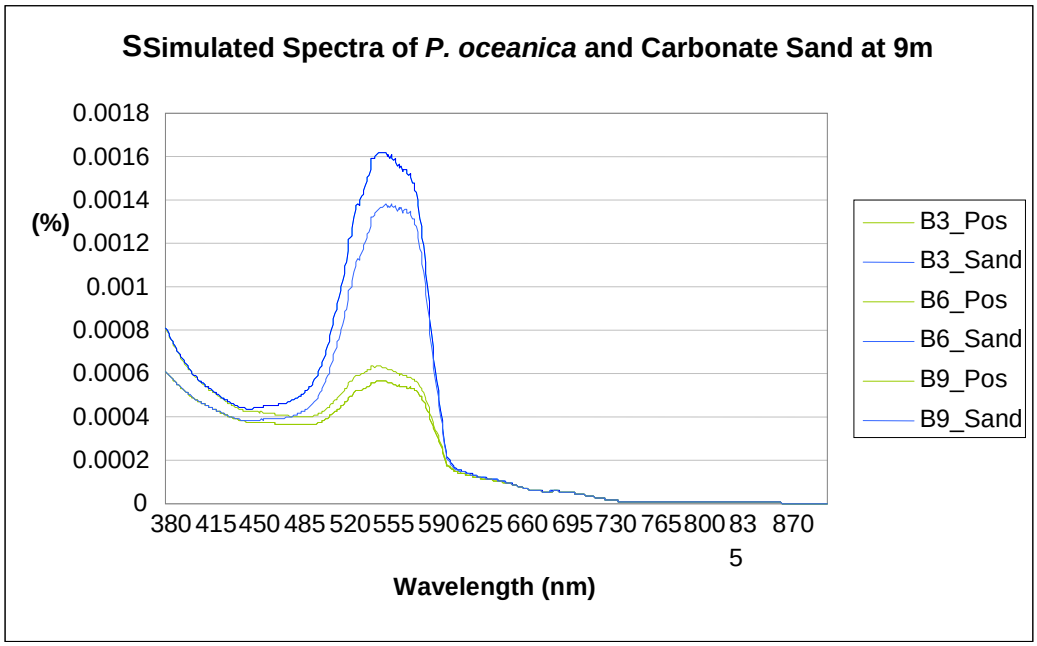

Figure 19: The parameters involved in the simulated spectra and its minimum and maximum values of reflectance of the seafloor types at 9m depth

When evaluating whether *P. oceanica* remains distinct within adverse conditions with increased CDOM, it resulted in a low reflectance value. For instance, at 4m depth when the CDOM was 0.10 m^{-1} the percent reflectance of the *P. oceanica* decreased by 3 percent with 4.4 % reflectance. The concentration CDOM (Gelbstoff) is a primary factor affecting the absorption on incident sunlight in coastal and estuarine waters. Hence may disrupt the abilities of mapping submerged vegetation when using remote sensing.

Table 7: The parameters involved in the simulated spectra and its minimum and maximum values of reflectance of the seafloor types at 9 m depth

	Parameters		*P. oceanica*		Sand	
Spectrum	Gelbstoff (m^{-1})	Depth (m)	Minimum	Maximum	Minimum	Maximum
B3	0.01	9	0.000002797	0.000806	0.000002797	0.00162
B6	0.03162	9	0.000002797	0.000608	0.000002797	0.00162
B9	0.1	9	0.000002797	0.000608	0.000002797	0.001383

4.7. Stepwise Discriminant for Spectral simulation

The multivariate stepwise discriminant analysis of the seafloor types within the depth of 4m produced a list of wavelengths that better discriminant the variables with a significance of 95%. (Stepwise statistics in Appendix 4) These selected wavelengths differ significantly between seafloor types.
Selected wavelengths: 445nm, and 485nm

However, the Wilk's lambda at 445nm is 0.924 and 485nm is 0.864. These values are near to 1 which indicates t hat the groups' means at these wavelength are not different. Eventhough, the

canonical function explains 100% of the variance; these values may cause some error when classifying as there is loss of signal and light penetration decreases.

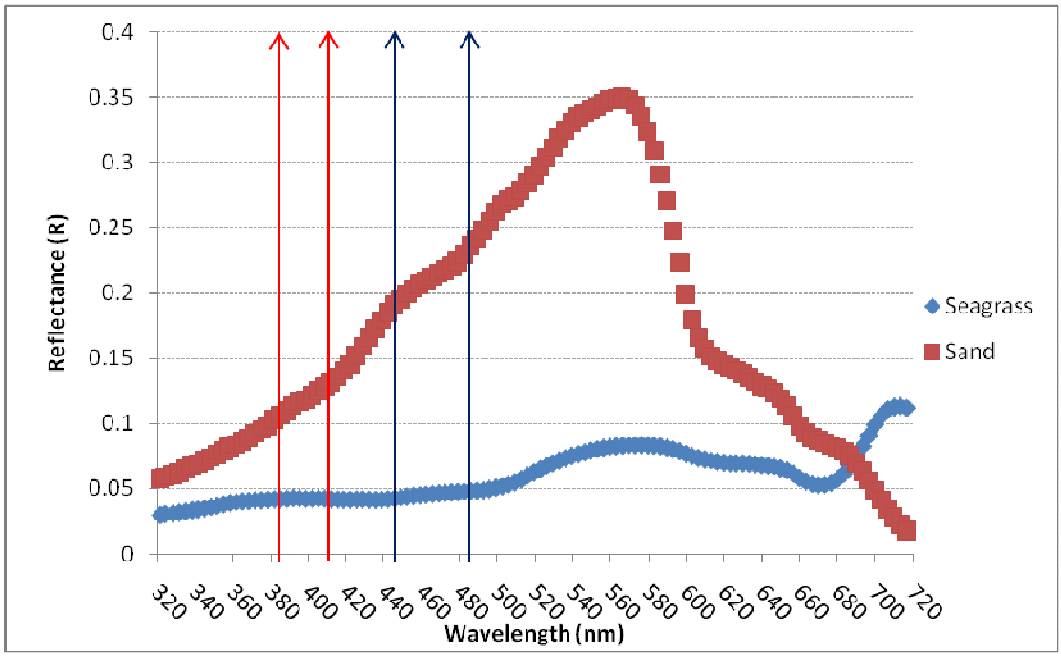

Figure 20: : Mean reflectance spectra of seafloor bottoms with selected bands for spectral discrimination for adverse conditions at 4m depth (blue lines) and 20 m depth (red lines)

To determine if *P. oceanica* was distinct under adverse condition, Stepwise discriminant analysis selected the following wavelengths at different depths. At the highest depth 20m, 3 wavebands were selected: 382 nm, 412 nm, and 773nm; whereas at 4 m, 445nm and 485 were chosen (Table 8). These are the wavelength at which *P. oceanica* is distinct in adverse conditions.

Table 8:Fisher's linear classification function coefficients at 4 m depth

Wavelength	Seafloor Type	
	Posidonia oceanica	Sand
4m		
445	434.358	1165.019
485	-316.630	-830.558
(Constant)	-1.831	-11.911
20m		
382	79.140	3041.947
412	-52.722	-1952.632
773	-13.399	-641.805
(Constant)	-.705	-22.653

5.Discussion

Spectral Discrimination of *in situ* spectral measurements

Monitoring the density and distribution of benthic vegetation is valuable for monitoring and management of coastal areas (Holden & Ledrew, 2003) as there is a critical requirement for information to promote and support ecosystem management (Phinn, 2006). The use of remote sensing methods for discriminating seagrass species can be a consistent and objective means in mapping large areas for monitoring purposes (Holden & Ledrew, 1998) but only if the spectra *in situ* species are distinct.

5.1. Spectral Description

The goal of this study was to determine whether underwater bottom reflectance measurements performed *in situ* close above patches of seagrass contain useful information for discrimination. A comprehensive library of two seafloor types was produced, where the spectral signatures of each seafloor type was produced.

The reflectance spectrum of the seagrass species, *P. oceanica* was found, and as expected, spectrally distinct from other seafloor types. In contrast to the other seafloor type, sand, *P. oceanica* displayed the absorption features characteristic of the spectral property of green plants that contain abundant chlorophyll. On the other hand, differences in the spectral signatures of seagrass *in situ* and laboratory as shown in Figure 10, was not so apparent. For example, at the green reflectance peak (540 – 560 nm) and the red absorption trough (670 – 680), they all exhibited the same spectral property of green plants. The reflectance difference is attributed to mainly to the presence of varying proportions and/or concentration of pigments such as *Chl a* and *Chl b* and a range xanthophylls and carotenes/ caroteniods (Gitelson et al., 2009; Merzlyak et al., 2003). In the blue region of the spectrum, absorption occurs from chlorophyll *a* and *b* and a range of caroteniods that extend absorption to shorter wavelengths of the visible spectrum (Blackburn, 1998). The influence of individual pigments on reflectance in the blue region cannot be observed in the spectral signatures of *P. oceanica*, thus the observed differences in the visible spectral reflectance between the *P. oceanica* and carbonate sand is attributed to the total and relative concentrations of chlorophyll, carotenoids and accessory pigments in their leaves. Additionally, in the blue wavelengths, remote sensing of benthic vegetation is impractical and because of sensor sensitivity is low, atmospheric effects are large and algal pigments, organic matter and detritus all absorb light.

Additional significant influences on the seagrass reflectance spectra are vegetation (patch) density, canopy openness and the amount form and orientation of leaves. The discrimination of *P. oceanica* using remote sensing relies upon differences in the magnitude if both pigment and structural characteristics as measured or seen in features of their absorption spectra (i.e. the depth and width of absorptions troughs or height and shape of reflectance peaks) (Durako, 2007). *P. oceanica* at Agia Pelagia grew from 1- 5m depth in a fairly uniform patches (1- 3 m diameter), thus accurate discrimination based on the moderate differences observed was feasible.

In studies of discrimination of terrestrial plant species, the largest differences in reflectance have been recorded in the near infrared (NIR) and shortwave infrared (SWIR) wavelength (Cho and

Skidmore, 2006; Cho et al., 2008; Skidmore et al., 2005; Sobhan, 2007). However, for the remote sensing of aquatic plants, it is limited to the visible wavelength where light penetrates the water column and reflected back to sensor. The effects of water column absorption are most noticeable at the wavelength longer than 720nm. Although NIR reflectance can be useful, the visible wavelengths (400 – 700 nm) are less attenuated by water column and thus were used. Therefore, the discrimination of spectral signatures of seagrass, *P. oceanica* species in comparison to sand were clearly distinct over wide regions of the visible wavelength of the spectrum as can be seen in Figure 10.

P. oceanica subsurface reflectance at 1.5 depths had slightly lower reflectance compared to Maltese 2008 study in both the visible and near infrared parts of spectrum as seen in Figure 11. There are a number of factors that contributed to the differences in reflectance. The presence and concentration of these photosynthetic and accessory pigments will vary because of genetic variation, seasonal cycles, stage of growth, health and environmental conditions (Alcoverro, 2001).
Furthermore, spatial and temporal variations in light and nutrient availability, as well as temperature, salinity and degree of water movement around plant will influence growth, photosynthesis and therefore the spectral response of the seagrass(Fyfe, 2003)

P. oceanica is a temperate seagrass and hence exhibit significant seasonal fluctuations controlled by factors such as solar energy, irradiance and temperature (Alcoverro et al., 2001; Marba et al., 1996). These factors play an important role in shallow environments where light availability is high. Previous studies demonstrated strong seasonality of *P. oceanica* growth with a summer maximum and a fall minimum (Alcoverro et al., 2001; Alcoverro et al., 1995). The seasonal fluctuations are demonstrated in the reflectance values of *in situ* measurement of *P. oceanica* taken in May, 2007 by Maltese and October, 2009. Thus it can be conclude that the difference in the reflectance value is because of the seasonal variability and the growth dynamics of this temperate species corresponding to the temporal variation aforementioned in relation to the availability of light.

Seagrass support a species rich community of epiphytic organisms. Epiphytes include a diverse array of micro algae, bacteria, juvenile macro-algae and sessile invertebrates. Epiphytes are likely to have an influence on above surface reflectance if present on leaf surfaces as they can mask reflection to an extent while contributing their own absorption and reflectance features to the spectral response (Fyfe, 2003; Fyfe and Davis, 2007; Maltese et al., 2007). In the patch of seagrass measured, there were leaves covered with epiphytes. However, the influence of presence of epiphytes on the presence was not considered. An assumption was that the percentage cover in the field of view of sensor was green leaves and the epiphyte covered leaves had a lower percentage and thus having little influence on the reflectance of *P. oceanica*.

Whereas, carbonate sand, had high reflectance values in comparison to the *P. oceanica* due to the presence of highly reflective calcium carbonate with a smooth ascending slope from short to long wavelength (Maritorena, 1996; Maritorena et al., 1994). However, the reflectance of carbonate sand in Figure 13 shows the combined effect of absorption by calcium carbonate sand grains and chlorophyll in benthic microalgae. The pigments existent within the microalgae is largely responsible for the spectral absorption and reflectance and determines the overall spectral shape of the reflectance (Hochberg et al., 2003; Stephens et al., 2003).

The effect of microalgal communities on the reflectance of carbonate sand in the shallow marine environments was evident in the spectral shape including dips at 678 nm for chlorophyll *a* and 478 nm for the caroteniods (Louchard et al., 2002; Louchard et al., 2003; Platt, 1995; Stephens et al., 2003). Reflectance could also be affected by the grain size (Hiroi and Pieters, 1992) with larger grains reflecting less light than smaller grains. Thus, the grain size might have been responsible for some of the difference in the magnitude of reflectance seen in Figure 13. Similarly, to *P. oceanica*, majority of the reflectance was lost when propagated through the water column.

5.2. Spectral Discrimnation Analysis

The application of spectroscopy in species discrimination is widespread both in the laboratory as well as field campaigns (Call et al., 2003; Schmidt and Skidmore, 2003; Sobhan, 2007). The high spectral resolution is useful for capturing and discriminating subtle differences in different targets. However this study has shown that spectral discrimination of submerged vegetation is a possibility. However, due to numerous bands available, there is redundant information at band level (Schmidt and Skidmore, 2003; Sobhan, 2007). Three statistical methods namely: Student's T test, ANOVA, and Spectral discriminant analysis was able to identify important sections of the spectrum to discriminate *P. oceanica* from carbonate sand.

The Student's T test was a method looks at each individual band separately to find the differences in each pair of combination between the *in situ* data and the laboratory data. The T test 162 bands had a p value less than 0.05 and so with 95% confidence the bands within the visible region of the spectrum were statistically significant between the two seafloor types indicating that they differ from one another. In the laboratory analysis the spectra were also statistically different in their spectral response. ANOVA test also tested the individual bands, but this time considering both *in situ* and laboratory data, where statistical significance was one again determined between pairs which was shown in Post Hoc Tukey test; whereas, the stepwise discriminant analysis is a selection process which considers the whole spectrum to identify the most discriminant band. These results not only indicate the potential to discriminate these seafloor types but also provide information about the bands that discriminate best.

The results clearly illustrate the relative importance of using different parts of the visible spectrum for discriminating the seafloor types. As a result, it can be hypothesised that spectral responses of leaf pigments contain more spectral information for discrimination. This is due to the presence of pigments in seagrass species and the lack thereof in carbonate sand. A relative comparison, with a study by (Hochberg and Atkinson, 2000) shows that although our results does not coincide fully with their findings, a general trend does exist. Moreover, these differences largely remain confined to the wavebands if the visible range of the spectrum.

The selected bands from the stepwise discriminant analysis demonstrate a distribution pattern along the wavelength: 328nm, 408nm, 445nm, 448nm, 482nm, 485nm, and 606nm demonstrate (1) the power of discrimination of these spectral regions without the involvement of algorithms (2) different methods may not identify exactly the same bands, but a similar discriminating band does exist within close proximity even in the adverse condition which may exist from one place to another. These bands selected had the highest number of frequency which is important in discriminating benthic/submerged environments.

The 52- and 14-wavelength subsets used in classification analyses

52-wavelength subset	14-wavelength subset
400, 401, 405, 406, 407, 409, 411, 417, 420, 421, 427, 429, 431, 434, 438, 441, 445, 451, 455, 457, 466, 470, 481, 497, 499, 508, 509, 528, 540, 541, 559, 565, 571, 576, 579, 585, 599, 601, 609, 611, 629, 639, 644, 651, 666, 670, 678, 679,	406, 430, 454, 467, 480, 499, 507, 529, 540, 577, 602, 608, 643, 684

Table 9: List of wavelength subsets identified by stepwise selection as those wavelengths without redundancy, provided the greatest separability used by Holden and Ledrew (2003) to classify coral reef bottom types including carbonate sand and seagrass.

5.3. Remote Sensing of *P. oceanica* using MERIS

The feasibility of advance technology has made it feasible to design a satellite sensor with the pourpose of addressing specific questions to in global protection of coastal zone ecosystems. The simulated spectrum was portrayed on a satellite sensor, Medium Resolution Imaging Spectrometer (MERIS). Some of the selected wavelengths for the spectral discrimination of *P. oceanica* coincided with the spectral bands of the MERIS sensor. Thus it can be used to map *P. oceanica* beds.

This sensor was designed for mapping oceanic components such as water constituents and other properties with the marine environment. However, it has the potential to map seagrass beds and the spectral bands correlate with the discriminant bands selected for *P. oceanica.* (See Appendix 7) *P. oceanica* meadows growing in very oligotrophic environments can be explained by the addition of two strategies: the high leaf longevity which allows a significant internal cycling of nutrients from senescent leaves, and the formation by the canopy of a nutrient rich water layer which largely increases the nutrient availability for the meadow during periods when nutrients are virtually absent of the column. Additionally the Cretan Sea is an extremely oligotrophic system. This conclusion was based on primary production rates whose reported values are among the lowest reported from the entire Mediterranean (Danovaro et al., 1994). The results of this study clearly confirm that there is extreme oligotrophy in the Cretan Sea. Additionally the most evident characteristic of this oligotrophic environment is the predominance of the smaller particles.

The parameters within the model were assumed to be the conditions of the Mediterranean Sea and it outputted spectral bands that are able to discriminate *P. oceanica* from other seafloor types. However, when classifying using the spectral bands, sub pixel needs to be taken into consideration. The MERIS sensor has pixel FOV of 0.019° whereas, the TRIOS has an FOV of 8.7cm and this may cause mixing of pixel as the magnitude of the pixel differ from the sensor used to collect the ground measurements. Therefore, ummixing methods for pixel will be relevant to map P oceanica using the MERIS sensor. Thus, high classification accuracies could be achieved for general bottom types such as *P. oceanica*.

5. Conclusion

This study was able to answer the research question: Is *P.oceanica* spectrally distinct from other seafloor types? The answer is yes. This study aimed to evaluate the spectral discrimination of *P. oceanica* from other seafloor type using Student t test, ANOVA and stepwise discriminant analysis. For the Student t test and ANOVA, *P. oceanica* was statistically significant from other seafloor types in the visible region of the spectrum. In addition, a better understanding has been gained about those parts of the electromagnetic spectrum that is relevant in mapping and detection submerged vegetation and seafloor types.

With high spectral resolution for imaging and non imaging spectroscopy discrimination of *P. oceanica* from other seafloor types is possible. Therefore, the TRIOS Ramses sensor was a reliable sensor, as it was able to detect the pigmentation of aquatic plants and is able to differentiate the seafloor bottoms.

The stepwise discriminant analysis found wavebands with the common regions in the spectrum with better discriminating properties. Thus, our results have shown that seven spectral wavebands of the visual spectrum yielded the highest discriminatory properties for *P. oceanica* at depth various depths.

In shallow and/or clear waters accurate reflectance of plants canopies measured *in situ* can be retrieved, providing that additional measurements of water column optical properties are also made using the WASI Model.

The WASI model was able to output simulated spectra of *P. oceanica* which remained spectrally distinct at varying depths and under adverse conditions.

This study has found that the measurement of any seafloor bottom is extremely repeatable. The reflectance measured *in situ* and in the laboratory was consistent in shape and magnitude with those reported by other researchers using a similar methodology (Hochberg & Atkinson, 2000; Holden and Ledrew, 1998, 1999; Maritorena et. al., 1994) attains bands with close proximity.

Remote sensing using the Medium Resolution Imaging Spectrometer (MERIS) is feasible as the bands selected corresponds to the spectral wavebands of the MERIS sensor. However to attain high classification accuracies, unmixing of sub pixel is necessary as the magnitude of the pixel between what is captured by the sensor and what is measured from the ground differ.

6. Recommendation

For this study, the stepwise discriminant analysis was used. I would recommend that derivative analysis be done to determine specific wavelength and compare them with this study.

The images that were provided from fieldwork were not feasible to use as the image did not consist of any seagrass beds. Thus I would recommend that a study be done to classify an image using the waveband selected using both the derivative and stepwise discriminant analysis. Then compare the accuracies of both maps.

More adverse conditions should be explored considering the suspended sediments at high levels in the water and determine the effect of suspended sediments on the effect of health and growth of *P. oceanica*.

7. References

Agostini S, Capiomont A, Marchand B, Pergent G. Distribution and estimation of basal area coverage of subtidal seagrass meadows in a Mediterranean coastal lagoon. Estuarine, Coastal and Shelf Science (2003) 56:1021-1028.

Albert A, Gege P. Inversion of irradiance and remote sensing reflectance in shallow water between 400 and 800 nm for calculations of water and bottom properties. Appl. Opt. (2006) 45:2331-2343.

Alcoverro T, Cerbian E, Ballesteros E. The photosynthetic capacity of the seagrass Posidonia oceanica: influence of nitrogen and light. Journal of Experimental Marine Biology and Ecology (2001) 261:107-120.

Alcoverro T, Duarte C, Romero J. Annual growth dyanmics of *Posidonia oceanica*: contribution of large scale versus local factors to seasonality. Mar. Ecol.-Prog. Ser. (1995) 120:203 - 210.

Allali K, Bricaud A, Babin M, Morel A, Chang P. A new method for measuring spectral absorption coefficients of marine particles. Limnology and Oceanography (1995) 40:1526-1532.

Andréfouët S, Muller-Karger FE, Hochberg EJ, Hu C, Carder KL. Change detection in shallow coral reef environments using Landsat 7 ETM+ data. Remote Sensing of Environment (2001) 78:150-162.

Andrefouet S, Robinson JA. The use of Space Shuttle images to improve cloud detection in mapping of tropical coral reef environments. International Journal of Remote Sensing (2003) 24:143 - 149.

Baden S, GullstrÃ¶m M, LundÃ©n B, Pihl L, Rosenberg R. Vanishing Seagrass (Zostera marina, L.) in Swedish Coastal Waters. AMBIO: A Journal of the Human Environment (2003) 32:374-377.

Bethoux JP, Copin-Montegut. Biological fixation of atmospheric nitrogen in the Mediteranean Sea. Limnology and Oceanography (1986) 31:1353-1358.

Birk RJ, McCord TB. Airborne hyperspectral sensor systems. In: Aerospace and Electronics Conference, 1994. NAECON 1994., Proceedings of the IEEE 1994 National (1994). 309-316 vol.301.

Blackburn GA. Quantifying Chlorophylls and Caroteniods at Leaf and Canopy Scales: An Evaluation of Some Hyperspectral Approaches. Remote Sensing of Environment (1998) 66:273-285.

Brando VE, Dekker AG. Satellite hyperspectral remote sensing for estimating estuarine and coastal water quality. Ieee Transactions on Geoscience and Remote Sensing (2003) 41:1378-1387.

Call KA, Hardy JT, Wallin DO. Coral reef habitat discrimination using multivariate spectral analysis and satellite remote sensing. International Journal of Remote Sensing (2003) 24:2627-2639.

Cho MA, Skidmore A, Corsi F, van Wieren SE, Sobhan I. Estimation of green grass/herb biomass from airborne hyperspectral imagery using spectral indices and partial least squares regression. International Journal of Applied Earth Observation and Geoinformation (2007) 9:414-424.

Cho MA, Skidmore AK. A new technique for extracting the red edge position from hyperspectral data: The linear extrapolation method. Remote Sensing of Environment (2006) 101:181-193.

Cho MA, Skidmore AK, Atzberger C. Towards red-edge positions less sensitive to canopy biophysical parameters for leaf chlorophyll estimation using properties optique spectrales des feuilles (PROSPECT) and scattering by arbitrarily inclined leaves (SAILH) simulated data. Int. J. Remote Sens. (2008) 29:2241-2255.

Clark CD. Satellite remote sensing for marine pollution investigations. Marine Pollution Bulletin (1993) 26:357-368.
Costanza R, et al. The value of the world's ecosystem services and natural capital. Nature (1997) 387:253-260.
Curran P. Imaging Spectrqmetry - Its Present And Future RÔLe In Environmental Research. In: Imaging Spectrometry — a Tool for Environmental Observations (1994). 1-23.
Danovaro R, Fabiano M, Boyer M. Seasonal changes of benthic bacteria in a seagrass bed (Posidonia oceanica) of the Ligurian Sea in relation to origin, composition and fate of the sediment organic matter. Mar Biol (1994) 119:489 - 500.
Dauby P. The stable carbon isotope ratios in benthic food webs of the gulf of Calvi, Corsica. Continental shelf Research (1989) 9:181-195.
Dekker AG, Brando VE, Anstee JM. Retrospective seagrass change detection in a shallow coastal tidal Australian lake. Remote Sensing of Environment (2005) 97:415-433.
Duarte C, Borun J, Short F, Walker DI. Seagrass Ecosystem: Their Global Staus and Prospects. In: Aquatic Ecosystems: Trends and Global Prospects--Polunin N, ed. (2008) Cambridge, United Kingdom: Cambridge University Press.
Duarte CM. Seagrass Depth Limits. Aquatic Botany (1991) 40:363-377.
Duarte CM. Submerged aquatic vegetation in relation to different nutirent regimes (1995). 87-112.
Duarte CM. The future of seagrass meadows. Environ. Conserv. (2002) 29:192-206.
Duarte CM, Marba N, Krause-Jensen D, Sanchez-Camacho M. Testing the predictive power of seagrass depth limit models. Estuaries and Coasts (2007) 30:652-656.
Durako MJ. Leaf optical properties and photosynthetic leaf absorptances in several Australian seagrasses. Aquatic Botany (2007) 87:83-89.
English DC, Carder KL. Determining Bottom Reflectance and Water Optical Properties Using Unmanned Underwater Vehicles under Clear or Cloudy Skies. Journal of Atmoshperic and Oceanic Technology (2005) 23:314-324.
Felipe J, et al. Flood Detection and Monitoring with autonomos science craft sexperiment onboard EO-1. Remote Sensing of Environment (2006) 101:463-481.
Ferwerda JG. Charting the Quality of Forage. Mapping and Measuring and Variation of Chemical Components in Foliage with Hyperspectral Remote Sensing. In: Natural Resource Management (2005) Enschede: ITC and Wageningen University. 166.
Foden J, Sivyer DB, Mills DK, Devlin MJ. Spatial and temporal distribution of chromophoric dissolved organic matter (CDOM) fluorescence and its contribution to light attenuation in UK waterbodies. Estuarine, Coastal and Shelf Science (2008) 79:707-717.
Fornes A, Basterretxea G, Orfila A, Jordi A, Alvarez A, Tintore J. Mapping Posidonia oceanica from IKONOS. ISPRS Journal of Photogrammetry and Remote Sensing (2006) 60:315-322.
Fourqurean JW, Robblee MB. Florida Bay: A history of recent ecological changes. Estuaries (1999) 22:345-357.
Freeman AS, Short FT, Isnain I, Razak FA, Coles RG. Seagrass on the edge: Land-use practices threaten coastal seagrass communities in Sabah, Malaysia. Biological Conservation (2008) 141:2993-3005.
Fyfe SK. Spatial and temporal variation in spectral reflectance: Are seagrass species spectrally distinct? Limnology and Oceanography (2003) 48:464-479.
Fyfe SK, Davis AR. Spatial scale and the detection of impacts on the seagrass Posidonia australis following pier construction in an embayment in southeastern Australia. Estuarine, Coastal and Shelf Science (2007) 74:297-305.
Garvey GF, John. The Rough Guide to Crete 7. (2007) 7 edn.: Rough Guides.
Gege P. The water color simulator WASI: an integrating software tool for analysis and simulation of optical *in situ* spectra. Computers & Geosciences (2004) 30:523-532.
Giraud G. Essai de classement des herbiers de Posidonia oceanica (Liine) Delile. Botanica Marina (1977) 20:487- 491.
Gitelson A, Merzlyak M. Signature Analysis of leaf reflectance spectra: algorithm development for remote sensing of chlorophyll. Journal of Plant Physiology (1996) 148:494 - 500.
Gitelson AA, Chivkunova OB, Merzlyak MN. Nondestructive estimation of anthocyanins and chlorophylls in anthocyanic leaves. Am. J. Bot. (2009) 96:1861-1868.

Glackin DL. International space-based remote sensing overview: 1980-2007
Canadian Journal of Remote Sensing
(1998) 24:307-314.
Gobert S, Cambridge ML, Velimirov B, Pergent G, Lepoint G, Bouquegneau JM. Biology of Posidonia. In: Seagrass: Biology, Ecology and Conservation--Larkum AWD, Orth RJ, Duarte C, eds. (2006) Berlin: Springer Verlag. 387-408.
Goetz AFH. Three decades of hyperspectral remote sensing of the Earth: A personal view. Remote Sensing of Environment (2009) 113:S5-S16.
Green EP, Mumby PJ, Edwards AJ, Clark CD. A review of remote sensing for the assessment and management of tropical coastal resources. Coast. Manage. (1996) 24:1-40.
Green RO, et al. Imaging Spectroscopy and the Airborne Visible/Infrared Imaging Spectrometer (AVIRIS). Remote Sensing of Environment (1998) 65:227-248.
Hays CG, Glen F, Broderick AC, Godley BJ, Metcalfe JD. Behavioral plasticity in a large marine herbivore: contrasting patterns of depth utilisation between two green turtle (*Chelonia mydas*) populations. Marine Biology (2002) 141:985-990.
Heege T, Fischer J. Mapping of water constituents in Lake Constance using multispectral airborne scanner data and a physically based processing scheme. Canadian Journal of Remote Sensing (2004) 30:77-86.
Hemminga M, Duarte, C. M. Seagrass Ecology (2000) Cambridge, UK: Cambrige University Press.
Hiroi T, Pieters CM. Effects of grain size and shape in modelling reflectance spectra of mineral miztures. Proceedings of Lunar and Planetary Science (1992) 22:313-325.
Hochberg EJ, Atkinson MJ. Spectral discrimination of coral reef benthic communities. Coral Reefs (2000) 19:164-171.
Hochberg EJ, Atkinson MJ, Andréfouët S. Spectral reflectance of coral reef bottom-types worldwide and implications for coral reef remote sensing. Remote Sensing of Environment (2003) 85:159-173.
Holden H, LeDrew E. Spectral Discrimination of Healthy and Non-Healthy Corals Based on Cluster Analysis, Principal Components Analysis, and Derivative Spectroscopy. Remote Sensing of Environment (1998) 65:217-224.
Holden H, LeDrew E. Effects of the water column on hyperspectral reflectance of submerged coral reef features. Bulletin of Marine Science (2001) 69:685-699.
Holden H, LeDrew E. Measuring and modeling water column effects on hyperspectral reflectance in a coral reef environment. Remote Sensing of Environment (2002) 81:300-308.
J. Cebrián, S. Enríquez, M. Fortes, N. Agawin, J. E. Vermaat, Duarte CM. Epiphyte Accrual on Posidonia oceanica (L.) Delile Leaves: Implications for Light Absorption. Botanica Marina (1999) 42:123-128.
Jerlov NG. Marine Optics. (1976).
Kamaruzaman J, Kasawani I. Hyperspectral Remote Sensing for Tropical Rainforest. American Journal of Applied Sciences (2009) 6:2001-2005.
Kelble C, Ortner P, Hitchcock G, Boyer J. Attenuation of photosynthetically available radiation (PAR) in Florida Bay: Potential for light limitation of primary producers. Estuaries and Coasts (2005) 28:560-571.
Kendrick GA, et al. Changes in seagrass coverage in Cockburn Sound, Western Australia between 1967 and 1999. Aquatic Botany (2002) 73:75-87.
Kendrick GA, Hegge BJ, Wyllie A, Davidson A, Lord DA. Changes in Seagrass Cover on Success and Parmelia Banks, Western Australia Between 1965 and 1995. Estuarine, Coastal and Shelf Science (2000) 50:341-353.
Kendrick GA, Marbà N, Duarte CM. Modelling formation of complex topography by the seagrass Posidonia oceanica. Estuarine, Coastal and Shelf Science (2005) 65:717-725.
Kutser T, Dekker AG, Skirving W. Modeling spectral discrimination of Great Barrier Reef benthic communities by remote sensing instruments. Limnology and Oceanography (2003) 48:497-510.
Larkum AWD, Orth RJ, Duarte C. Seagrass: Ecology. (2006) Dordrecht, the Netherlands: Springer.

Lehmann EL. Nonparametrics: statistical methods based on ranks, revised first edition--Hall P, ed. (1998) Upper Saddle River.
Leriche A, et al. Spatial, temporal and structural variations of a Posidonia oceanica seagrass meadow facing human activities. Aquatic Botany (2006) 84:287-293.
Lewotsky K. Hyperspectral Imaging: Evolution of Imaging Spectrometry. In: Optical Engineering--Report O, ed. (1994).
Louchard EM, et al. Derivative analysis of absorption features in hyperspectral remote sensing data of carbonate sediments. Optics Express (2002) 10:1573-1584.
Louchard EM, Reid RP, Stephens FC, Davis CO, Leathers RA, Downes TV. Optical remote sensing of benthic habitats and bathymetry in coastal environments at Lee Stocking Island, Bahamas: A comparative spectral classification approach. Limnology and Oceanography (2003) 48:511-521.
Maltese A, Pampalone V, Malthus TJ, Ciraolo G, Karpouzli E, La Loggia G. Processing of Field Spectroradiometric data for remote sensing mapping of submerged vegetation in coastal zone and lagoon environments. In: Remote Sensing of Coastal Zone: from Inland to Marine Waters (2007) Bolzano, Italy.
Malthus TJ, Mumby PJ. Remote sensing of the coastal zone: an overview and priorities for future research. International Journal of Remote Sensing (2003) 24:2805 - 2815.
Marba, et al. Direct Evidence of Imbalanced Seagrass (Posidonia oceanica) Shoot Population Dynamics in the Spanish Mediterranean. Estuaries (2005) 28:53-62.
Marba N, Duarte CM. Rhizome elongation and seagrass clonal growth. Mar. Ecol.-Prog. Ser. (1998) 174:269-280.
Marba N, Duarte CM, Cebrian J, Gallegos ME, Olesen B, SandJensen K. Growth and population dynamics of Posidonia oceanica on the Spanish Mediterranean coast: Elucidating seagrass decline. Mar. Ecol.-Prog. Ser. (1996) 137:203-213.
Maritorena S. Remote sensing of the water attenuation in coral reefs: A case study in French Polynesia. International Journal of Remote Sensing (1996) 17:155-166.
Maritorena S, Morel A, Gentili B. Diffuse reflectance of oceanic shallow waters - influence of water depth and bottom albedo. Limnology and Oceanography (1994) 39:1689-1703.
Mateo MA, Romero J, Perez M, Littler MM, Littler DS. Dynamics of millenary organic deposits resulting from the growth of the Mediterranean seagrass Posidonia oceanica. Estuarine Coastal and Shelf Science (1997) 44:103-110.
McWire K, Minor T, Fenstermaker L. Hyperspectral mixture modelling for quantifying sparse vegetation cover in arid environments. Remote Sensing of Environment (2000) 72:360 - 374.
Merzlyak MN, Gitelson AA, Chivkunova OB, Solovchenko AE, Pogosyan SI. Application of Reflectance Spectroscopy for Analysis of Higher Plant Pigments. Russian Journal of Plant Physiology (2003) 50:704-710.
Mobley C. Light and Water: radiative transfer in natural waters. (1994) San Diego: Academic Press.
Morel A, Claustre H, Antoine D, Gentili B. Natural variability of bio-optical properties in Case 1 waters: attenuation and reflectance within the visible and near-UV spectral domains, as observed in South Pacific and Mediterranean waters. Biogeosciences (2007) 4:913-925.
Mumby PJ, et al. Remote sensing of coral reefs and their physical environment. Marine Pollution Bulletin (2004) 48:219-228.
Pacheco A, Bannari A, Staenz K, McNairn H. Deriving percent crop cover over agriculture canopies using hyperspectral remote sensing. Canadian Journal of Remote Sensing (2008) 34.
Pasqualini V, Pergent-Martini C, Clabaut P, Pergent G. Mapping ofPosidonia oceanicausing Aerial Photographs and Side Scan Sonar: Application off the Island of Corsica (France). Estuarine, Coastal and Shelf Science (1998) 47:359-367.
Pasqualini V, Pergent-Martini C, Pergent G. Environmental impact identification along the Corsican coast (Mediterranean sea) using image processing. Aquatic Botany (1999) 65:311-320.
Pasqualini V, et al. Use of SPOT 5 for mapping seagrasses: An application to Posidonia oceanica. Remote Sensing of Environment (2005) 94:39-45.

Phinn S, Roelfsema C, Dekker A, Brando V, Anstee J. Mapping seagrass species, cover and biomass in shallow waters: An assessment of satellite multi-spectral and airborne hyper-spectral imaging systems in Moreton Bay (Australia). Remote Sensing of Environment (2008) 112:3413-3425.

Piazzi L, Acunto S, Cinelli F. Mapping of Posidonia oceanica beds around Elba Island (western Mediterranean) with integration of direct and indirect methods. Oceanologica Acta (2000) 23:339-346.

Platt T. Light and photosynthesis in aquatic systems : By J.T.O. Kirk, 2nd edition; Cambridge University Press, Cambridge; 1994; 509 pp.; GBP 50.00, US$ 84.95 (hard back); GBP 22.95, US$ 34.95 (paperback); ISBN 0-521-45353-4 (hardback), 0-521-45966-4 (paperback). Journal of Experimental Marine Biology and Ecology (1995) 185:133-134.

R. J. Orth DJW, L. S. Nagey, A. L. Owens, J. R. Whiting, and A. Kenne. Distribution of submerged aquatic vegetation in the Chesapeake Bay. In: VIMS Special Scientific Report (2006) Washington, D.C: Virgina Institute of Marine Sciences.

Ralph PJ, Durako MJ, Enríquez S, Collier CJ, Doblin MA. Impact of light limitation on seagrasses. Journal of Experimental Marine Biology and Ecology (2007) 350:176-193.

Rencher AC. Methods of Mutivariate Analysis. (1995) New York: Wiley.

Richardson LL, LeDrew EF, Gege P. Remote sensing of aquatic coastal ecosystem processes : science and management applications. (2006) Dordrecht: Springer.

Schmidt K. Hyperspectral remote sensing of Vegetation Species Distribution in a Saltmarsh. In: Natural Resource Management (2003) Enschede: ITC and Wageningen University. 252.

Schmidt KS, Skidmore AK. Spectral discrimination of vegetation types in a coastal wetland. Remote Sensing of Environment (2003) 85:92-108.

Scott AS. Bottom Albedo Derivations using Hyperspectral Spectrometry and Multispectral Video. In: Marine Science (2005): University of South Florida. 71.

Shafique N, Autrey F, Cormier S, Fulk F. Hyperspectral narrow wavebands selection for optimising water quality monitoring on the Great Miami River, Ohio. Journal of Spatial Hydrology (2001) 1:1-22.

Short FC, Robert G. (eds). Global Seagrass Research Methods (2001) Amsterdam: Elselvier Science B.V. 506.

Short FT, Wyllie-Echeverria S. Natural and human-induced disturbance of seagrasses. Environ. Conserv. (1996) 23:17-27.

Silio-Calzada A, Bricaud A, Uitz J, Gentili B. Estimation of new primary production in the Benguela upwelling area, using ENVISAT satellite data and a model dependent on the phytoplankton community size structure. Journal of Geophysical Research-Oceans (2008) 113.

Simms, Eacute, L, Dubois JMM. Satellite remote sensing of submerged kelp beds on the Atlantic coast of Canada. International Journal of Remote Sensing (2001) 22:2083-2094.

Skidmore AK, Mutanga O, Schmidt KS, Ferwerda JG. Modelling herbivore grazing resources using hyperspectral remote sensing and GIS. In: AGILE 2005 : proceedings of the 8th conference on geographic information science, July 24-29, 2005, Denver, U.S.A. / ed. by F. Toppen and M. Painho. Lisboa: AGILE, Universidade Nova de Lisboa, 2005. pp. 223-230 (2005).

Sobhan MI. Species Discrimination from a Hyperspectral Perspective. In: Natural Resource Management (2007) Enschede: ITC and Wageningen University. 176.

Stephens FC, Louchard EM, Reid RP, Maffione RA. Effects of microalgal communities on reflectance spectra of carbonate sediments in subtidal optically shallow marine environments. Limnology and Oceanography (2003) 48:535-546.

Underwood E, Ustin SL, Dipiertro D. Mapping non-native plants using hyperspectral imagery. Remote Sensing of Environment (2003) 86:150-161.

Vahtmae E, Kutser T, Martin G, Kotta J. Feasibility of hyperspectral remote sensing for mapping benthic macroalgal cover in turbid coastal waters - a Baltic Sea case study. Remote Sensing of Environment (2006) 101:342-351.

Vane G, Goetz AFH. Terrestrial imaging spectroscopy. Remote Sensing of Environment (1988) 24:1-29.

Vela A, et al. Use of SPOT 5 and IKONOS imagery for mapping biocenoses in a Tunisian Coastal Lagoon (Mediterranean Sea). Estuarine, Coastal and Shelf Science (2008) 79:591-598.

Wabnitz CC, Andréfouët S, Torres-Pulliza D, Müller-Karger FE, Kramer PA. Regional-scale seagrass habitat mapping in the Wider Caribbean region using Landsat sensors: Applications to conservation and ecology. Remote Sensing of Environment (2008) 112:3455-3467.

Waycott M, et al. Accelerating loss of seagrasses across the globe threatens coastal ecosystems. Proc. Natl. Acad. Sci. U. S. A. (2009) 106:12377-12381.

Yang D, Yang C. Detection of Seagrass Distribution Changes from 1991 to 2006 in Xincun Bay, Hainan, with Satellite Remote Sensing. Sensors (2009) 9:830-844.

8. Appendices

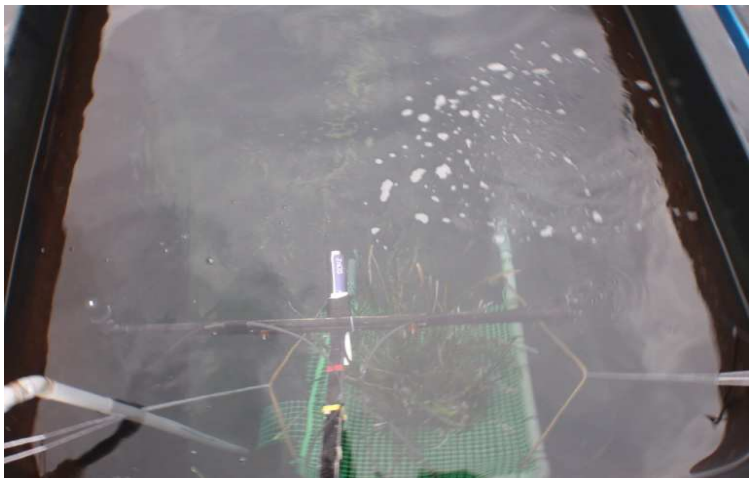

Appendix 1: The Institute of Aquaculture, HMCR, Crete Greece. The laboratory measurement was carried out. (B) The set up and the data collection of spectral measurements of *P. oceanica*

Appendix 2: Table of Parameter used in the WASI Model

Symbol	WASI	Units	Description
C_i	C[i]	ug l^{-1}	Concentration of phytoplankton class
C_L	C_L	mg l^{-1}	Concentration of small particles
C_S	C_S	mg l^{-1}	Concentration of small suspended particles
X	C_X	m^{-1}	Concentration of non-chlorophyllous particles
Y	C_Y	M^{-1}	Concentration of Gelbstoff
S	S	Nm^{-1}	Exponent of Gelbstoff Absorption
n	n	-	Exponent of backscattering by small particles
T	T_W	°C	Water Tempreture
f	*f*		Proportionality factor of reflectance ("*f* factor)
Q	Q	sr	Anisotropy factor ("Q factor")
θ_{sun}	Sun	°	Sun zenith angle
θ_{view}	View	°	View angle (0 = nadir)
σ	Sigma_L	-	Reflection factor of sky radiance
ν	Nue		Exponent of aerosol scattering
α	Alpha	-	Fraction of irradiance due to direct solar radiation
β	Beta	-	Fraction of irradiance due to molecule scattering
γ	Gamma	-	Fraction of irradiance due to aerosol scattering
δ	Delta	-	Fraction of irradiance due to cloud scattering
α*	Alpha_s	sr^{-1}	Fraction of radiance due to direct solar radiation
β*	Beta_s	sr^{-1}	Fraction of radiance due to molecule scattering
γ*	Gamma_s	sr^{-1}	Fraction of radiance due to aerosol scattering
δ*	Delta_s	sr^{-1}	Fraction of radiance due to cloud scattering
f_n	f (A)	-	Areal fraction of bottom surface types no. n = 0

Appendix 3: Tables from the discriminant analysis for the spectral library of seafloor bottoms

Stepwise Statistics

Variables Entered/Removed[a,b,c,d]

Step	Entered	Removed	Wilks' Lambda							
							Exact F			
			Statistic	df1	df2	df3	Statistic	df1	df2	Sig.
1	448		.277	1	1	164.000	428.440	1	164.000	.000
2	736		.159	2	1	164.000	432.110	2	163.000	.000
3	849		.129	3	1	164.000	364.568	3	162.000	.000
4	482		.120	4	1	164.000	295.650	4	161.000	.000
5	408		.082	5	1	164.000	357.145	5	160.000	.000
6	318		.077	6	1	164.000	315.725	6	159.000	.000
7		849	.078	5	1	164.000	378.442	5	160.000	.000
8	856		.074	6	1	164.000	330.177	6	159.000	.000
9	328		.071	7	1	164.000	293.554	7	158.000	.000
10		318	.072	6	1	164.000	343.994	6	159.000	.000
11	952		.069	7	1	164.000	304.999	7	158.000	.000
12	606		.066	8	1	164.000	277.718	8	157.000	.000
13	786		.064	9	1	164.000	252.729	9	156.000	.000

At each step, the variable that minimizes the overall Wilks' Lambda is entered.

a. Maximum number of steps is 384.

b. Minimum partial F to enter is 3.84.

c. Maximum partial F to remove is 2.71.

d. F level, tolerance, or VIN insufficient for further computation.

Appendix 4: Tables from the discriminant analysis for the spectral library of seafloor bottoms at 4m

Step		Tolerance	F to Remove	Wilks' Lambda
1	@445	1.000	5.743	
2	@445	.003	5.389	.931
	@485	.003	4.815	.924

Variables Entered/Removed[a,b,c,d]

Step	Entered	Wilks' Lambda							
						Exact F			
		Statistic	df1	df2	df3	Statistic	df1	df2	Sig.

1	@445	.924	1	1	70.000	5.743	1	70.000	.019
2	@485	.864	2	1	70.000	5.436	2	69.000	.006

At each step, the variable that minimizes the overall Wilks' Lambda is entered.

a. Maximum number of steps is 320.

b. Minimum partial F to enter is 3.84.

c. Maximum partial F to remove is 2.71.

d. F level, tolerance, or VIN insufficient for further computation.

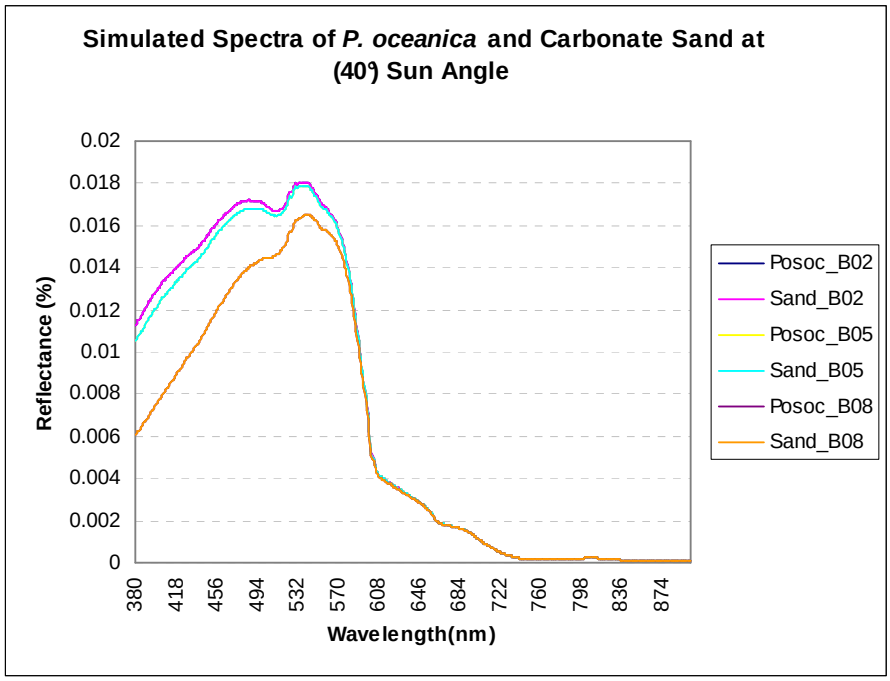

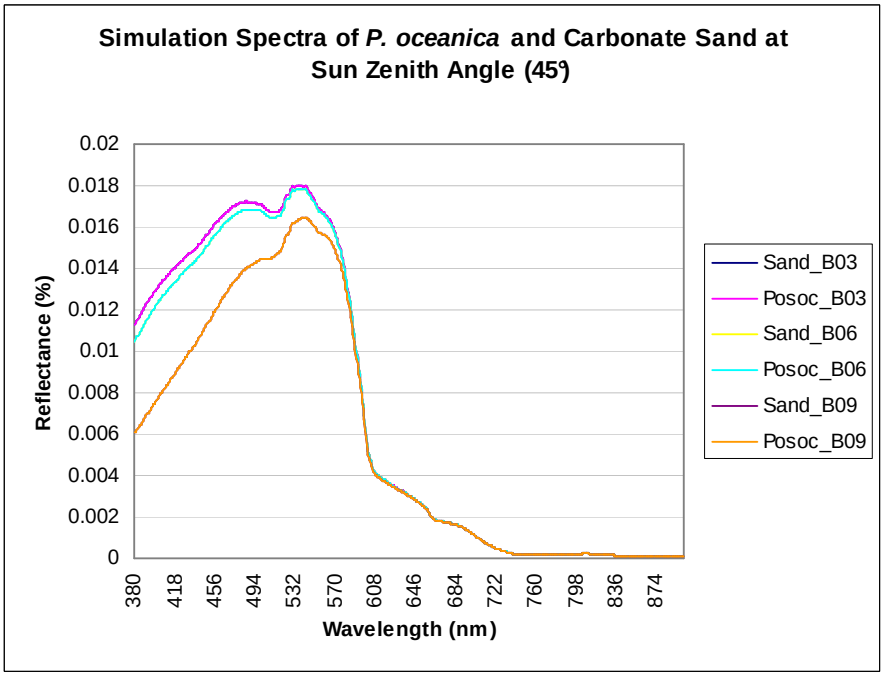

	Parameters		*P. oceanica*		Carbonate Sand	
Spectrum	Gelbstoff (m^{-1})	Sun Zenith Angle (°)	Minimum	Maximum	Minimum	Maximum
B2	0.01	40	0.00006841	0.0186	0.00006841	0.07186
B5	0.055	40	0.00006841	0.01789	0.00006841	0.01789
B8	0.01	40	0.00006841	0.01656	0.00006841	0.01656
B3	0.01	45	0.00006867	0.018	0.00006867	0.018
B6	0.055	45	0.00006867	0.01784	0.00006867	0.01784
B9	0.01	45	0.00006867	0.01649	0.00006867	0.01649

Appendix 5: The graph and parameters of simulated spectra of *P. oceanica* and Carbonate sand at 40 and 45 °SZA

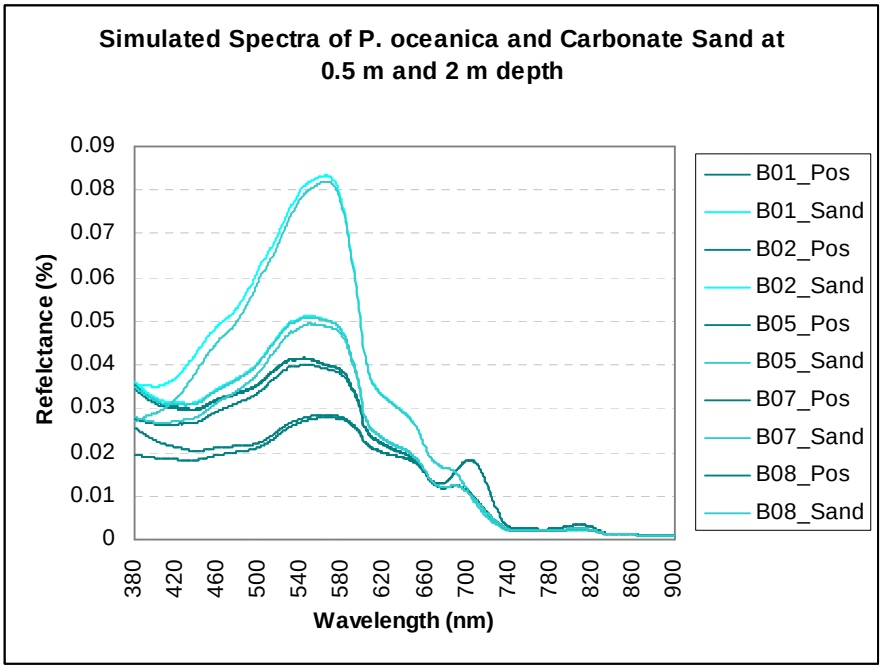

	Parameters		*P. oceanica*		Carbonate Sand	
Spectrum	Gelbstoff	Depth	Minimum	Maximum	Minimum	Maximum
B01	0.01	0.5	0.000707	0.02846	0.000705	0.08334
B02	0.01	2.25	0.000703	0.04166	0.000703	0.0512
B04	0.055	0.5	0.000707	0.02817	0.000705	0.08266
B05	0.055	2.25	0.000703	0.0415	0.000703	0.05101
B07	0.1	0.5	0.000707	0.02788	0.000705	0.08199
B08	0.1	2.25	0.000703	0.04013	0.000703	0.04933

Appendix 6: The Graph and Table showing the conditions of Simulated spectra at 1.5 m depth .

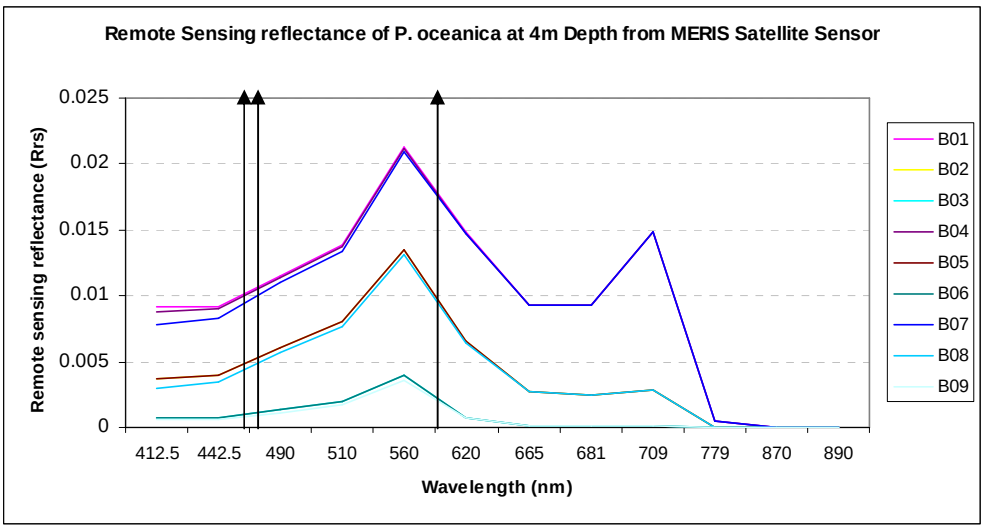

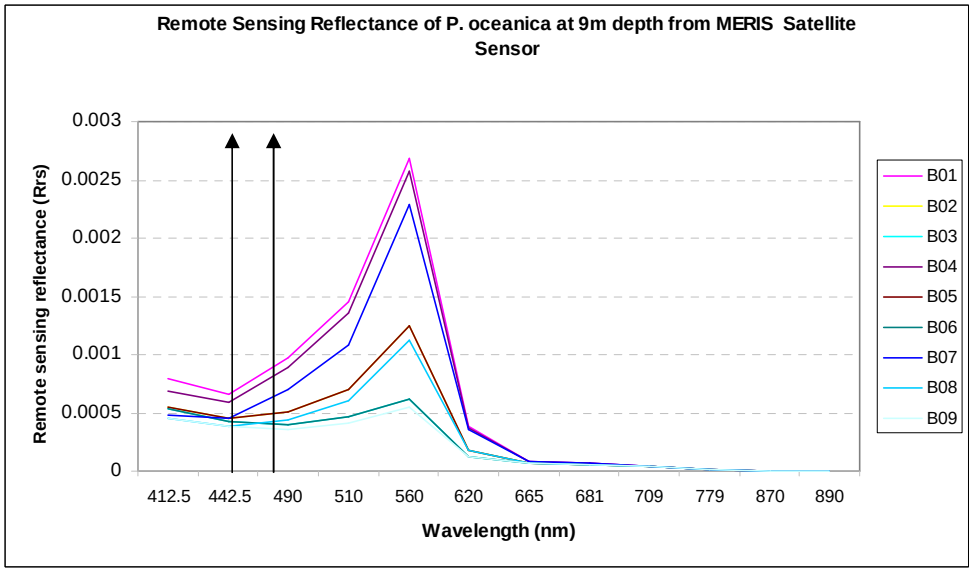

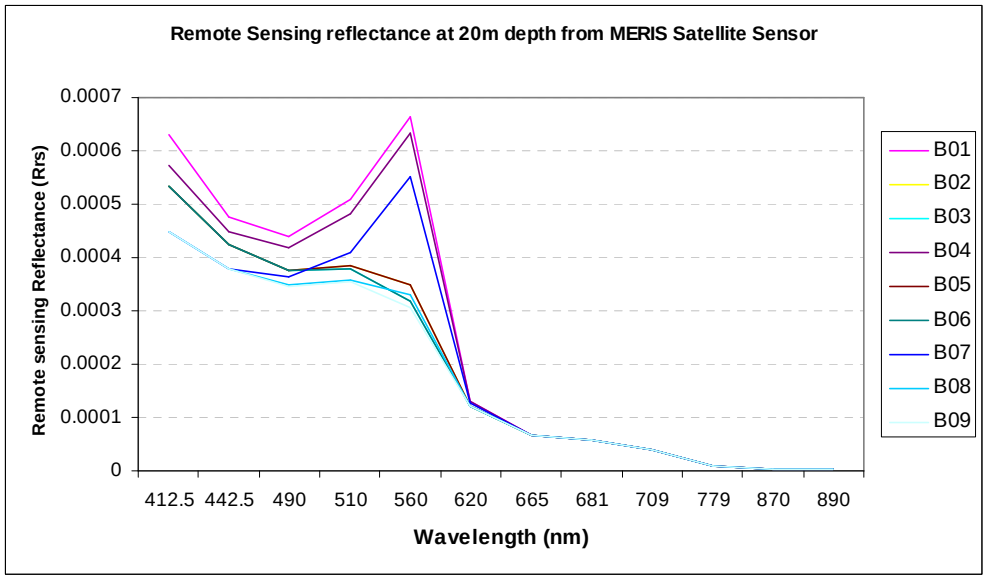

Appendix 7: Remote sensing reflectance of *P. oceanica* at varying depths with the wavebands selection from the Stepwise discriminate function analysis.